Modeled sensitivity of Lake Michigan productivity and zooplankton to changing nutrient concentrations and quagga mussels

Darren J. Pilcher [1,2], Galen A. McKinley [1,3,4], James Kralj [1,5], Harvey A. Bootsma [6], Euan D. Reavie [7]

[1] Department of Atmospheric and Oceanic Sciences, University of Wisconsin-Madison, Madison, WI, USA.

[2] NOAA Pacific Marine Environmental Laboratory, NOAA, 7600 Sand Point Way NE, Seattle WA 98115 USA.

[3] Center for Climatic Research, University of Wisconsin-Madison, Madison, WI, USA.

[4] Now at Columbia University / Lamont Doherty Earth Observatory, Palisades, NY 10964, USA.

[5] School of Marine and Environmental Affairs, University of Washington, Seattle, Washington, USA.

[6] School of Freshwater Sciences, University of Wisconsin-Milwaukee, Milwaukee, WI, USA.

[7] Natural Resources Research Institute, University of Minnesota Duluth, Duluth, MN, USA.

Corresponding author: Darren J. Pilcher (darren.pilcher@noaa.gov, 206-526-6055)

Key Points

- Simulate the impact of quagga mussels and reduced nutrients on lakewide productivity
- Quagga mussels are the dominant driver during periods of vertical mixing, while nutrients are dominant during stratification
- Both processes are required to capture observed decadal decline in Lake Michigan productivity

Abstract

The recent decline in Lake Michigan productivity is often attributed to filter feeding by invasive quagga mussels, but some studies also implicate reductions in lake-wide nutrient concentrations. We use a 3D coupled hydrodynamic - biogeochemical model to evaluate the effect of changing nutrient concentrations and quagga mussel filtering on phytoplankton production and phytoplankton and zooplankton biomass. Sensitivity experiments are used to assess the net effect of each change separately and in unison. Quagga mussels are found to have the greatest impact during periods of isothermal mixing, while nutrients have the greatest impact during thermal stratification. Quagga mussels also act to enhance spatial heterogeneity, particularly between nearshore-offshore regions. This effect produces a reversal in the gradient of nearshore-offshore productivity: from relatively greater nearshore productivity in the pre-quagga lake to relatively lesser nearshore productivity after quaggas. The combined impact of both processes drives substantial reductions in phytoplankton and zooplankton biomass, as well as significant modifications to the seasonality of surface water pCO_2, particularly in nearshore regions where mussel grazing continues year-round. These results support growing concern that considerable losses of phytoplankton and zooplankton will yield concurrent losses at higher trophic levels. Comparisons to observed productivity suggest that both quagga mussel filtration and lower lakewide total phosphorus are necessary to accurately simulate recent changes in primary productivity in Lake Michigan.

Keywords: large lakes, Dreissena, biogeochemical modeling, nutrient cycling, Great Lakes

1. *Introduction*

The Laurentian Great Lakes have an extensive history of ecological transformations due to anthropogenic activities. River inputs of phosphorus from agricultural runoff and detergents have significantly declined in recent decades but are still sufficient to promote eutrophication and extensive harmful algal blooms in some areas [*Michalak et al.,* 2013]. Invasive species, often transported incidentally via ships from the Great Lakes canal system, have displaced many native species and re-engineered the food web [*Cuhel and Aguilar* 2013], with significant impacts to valuable ecosystem services [*Rothlisberger et al.,* 2012]. Other stressors such as mercury contamination and hypoxia contribute to a total of 50 identified anthropogenic stressors with varying lakewide impacts [*Smith et al.,* 2015]. Climate change is associated with warming and loss of lake ice [*Mason et al.* 2016], which may have direct and indirect effects on phytoplankton production and nutrient cycling. CO_2 induced lake acidification is another potential threat with unknown biological impacts [*Phillips et al.,* 2015].

Lake Michigan is the 2nd largest of the Laurentian Great Lakes by volume, with an average depth of 85 meters and a water flushing time of 105 years [*Bootsma and Hecky* 2003]. The Great Lakes Water Quality Agreement of 1978 set targets for phosphorus loading limits, in order to reduce nuisance algae blooms associated with lake eutrophication. Because phosphorus is the limiting nutrient in Lake Michigan, this bottom-up strategy was viewed as the most direct avenue for reducing nearshore productivity. The imposed limits led to an observable decrease in total phosphorus concentrations by the mid-1990s [*Barbiero et al.,* 2002], along with a decline in the seasonal drawdown of silica, taken as indirect evidence of a decline in productivity [*Evans et al.,* 2011]. However, several studies were unable to elucidate a significant decline in offshore chlorophyll concentrations, despite the decrease in phosphorus loading [*Fahnenstiel and Scavia*

1987; *Johengen et al.,* 1994]. Thus, the impact of phosphorus inputs on offshore phytoplankton is relatively unclear.

While phosphorus loading and the effect on primary productivity continues to be an area of active research (e.g. *Stow* 2015; *Warner and Lesht* 2015), there has also been considerable effort to determine the ecological impacts associated with invasive species. The most recent Lake Michigan ecosystem transition occurred following the arrival of invasive *Dreissena* mussels. Zebra mussels (*Dreissena polymorpha*) were first documented in Lake Michigan in 1987 and established significant nearshore populations by the late 1990s [*Nalepa et al.,* 1998; *Bunnell et al.,* 2014]. A decline in primary productivity and increase in water transparency were observed immediately following the arrival of zebra mussels in Saginaw Bay and Lake Erie [*Fahnenstiel et al.,* 1995; *Nicholls and Hopkins* 1993], yet similar impacts were never fully realized in Lake Michigan. This lack of detection may be attributable to the spatial extent of the zebra mussel expansion, with mussels largely confined to nearshore regions, as compared to the locations of time series data at the offshore locations used for EPA and NOAA long-term ecosystem monitoring. Furthermore, concurrent declines in phosphorus loading were anticipated to produce the same effects as the zebra mussels (e.g. decline in primary productivity and increase in water clarity), making attribution difficult. Ultimately, the long-term response may have never been fully realized due to the short timeframe of zebra mussel establishment prior to elimination by competing quagga mussels (*Dreissena rostriformis bugensis*).

Quagga mussels were first reported in Lake Michigan in 1997 and have subsequently expanded throughout both the nearshore and offshore [*Nalepa et al.,* 2010; *Bunnell et al.,* 2014]. Quagga mussels out-compete zebra mussels due to their abilities to settle on both hard and soft substrate, to devote less energy to respiration and more energy to assimilation and growth, and to

graze at colder water temperatures [*Baldwin et al.,* 2002]. These advantages have enabled quagga mussels to effectively eliminate zebra mussels from Lake Michigan. Quagga mussel densities are substantially greater than previous maximum zebra mussel densities, and are established at depths that were unattainable by zebra mussels [*Nalepa et al.,* 2010]. Recent samplings show that populations at depths less than 50m appear to have leveled off, though densities at the deepest locations (>90m) continue to increase [*Nalepa et al.,* 2014].

This shift in mussel population composition and density correlates with a significant drop in spring primary productivity [*Fahnenstiel et al.,* 2010] and a disappearance in the late-winter phytoplankton bloom [*Kerfoot et al.,* 2010]. The overall decline in productivity has transformed the historically mesotrophic southern basin into an oligotrophic system, similar to Lake Superior [*Mida et al.,* 2010]. There is also evidence that *Dreissena* mussels have re-engineered nearshore-offshore phosphorus dynamics by sequestering phosphorus in the nearshore benthos, a process referred to as the "nearshore phosphorus shunt" [*Hecky et al.,* 2004; *Waples et al.,* 2017]. This buildup of nearshore benthic phosphorus in addition to increased light penetration is likely responsible for a substantial increase in nearshore *Cladophora* blooms as well as a contributing factor of the observed decline in offshore total phosphorus concentrations [*Bootsma et al.,* 2012]. This mechanism creates a difficult management scenario where nearshore water quality is substantially reduced due to *Cladophora* blooms, while offshore waters become oligotrophic, with negative impacts to higher trophic organisms and fisheries.

Recent evidence suggests that the transition to this eutrophic nearshore but oligotrophic offshore state is already underway. *Turschak et al.,* [2014] found that, following the arrival of quagga mussels, pelagic fish are becoming more reliant on nearshore energy subsidies. A substantial decline in offshore zooplankton populations, despite a concurrent decline in

planktivorous fish, suggests that a bottom-up control mechanism such as quagga mussel grazing is primarily responsible [*Pothoven and Fahnenstiel* 2014]. However, *Madenjian et al.,* [2015] find that predatory fish have remained relatively abundant despite the decline in primary productivity and zooplankton, suggesting the influence of additional factors.

The evidence tying the decline in primary productivity to quagga mussels is based on (1) the timing of the decline occurring immediately following establishment of quagga mussels, (2) the seasonal nature of the decline (i.e. most significant drop in productivity occurs during isothermal mixing when surface waters interact with benthos), and (3) the lack of a sufficient alternate explanation. Points (1) and (3) are supported by the abrupt timing of the decline in spring productivity, because it has been argued that other potential causes such as phosphorus loading or climate change cannot produce the observed magnitude of change within just a couple years [*Fahnenstiel et al.,* 2010]. Point (2) provides a mechanistic explanation for the response as well as a useful fingerprint to attribute the decline in productivity to the mussels (i.e. decline in spring productivity but no net change in summer productivity). Given the multiple interacting processes, a coupled physical-biogeochemical model can be a useful tool for developing and testing mechanistic links and for separating the effects of concurrent processes via sensitivity simulations. A recent modeling study was able to successfully capture observed spring productivity by parameterizing productivity as a function of light and temperature, and including a mussel grazing term [*Rowe et al.,* 2015a]. However, the model was less successful at simulating summer productivity, which the authors attribute to their model not including nutrients as a limiting factor for phytoplankton growth. Here, we utilize a 3D computational model to test both the impact of quagga mussels and changing nutrient concentrations on primary productivity and zooplankton population.

2. Methods

2.1 The Model

We use a 3D hydrodynamic model (Figure 1) coupled to an intermediate complexity ecosystem model, previously utilized for Lake Michigan (MITgcm.Michigan; *Pilcher et al.,* 2015). Briefly, the hydrodynamic model uses atmospheric forcing from the North American Regional Reanalysis Project (NARR) over a 2007-2010 timeframe, with lake ice imposed from observations (*Mesinger et al.,* 2006; U.S. National Ice Center 2010). The model compares favorably to observations of surface water temperature from two offshore buoys, with annual root mean square error (RMSE) values of 1.92°C and 2.13°C. The model also captures spatial variability in surface temperature, including the seasonal development of coastal upwelling along the western shoreline [Pilcher et al., 2015]. However, the model does contain a consistent warm bias, which results from a warm bias in the NARR forcing product and the use of prescribed rather than simulated lake ice coverage [*Bennington et al.,* 2010; *Rowe et al.,* 2015a]. This results in the model stratifying approximately 1 month earlier than observed [*Pilcher et al.,* 2015].

The ecosystem model contains two phytoplankton groups (small and diatom) and one zooplankton group (Figure 2). Phytoplankton growth is calculated based on Michaelis-Menton type parameterizations for light and nutrient limitation, along with a temperature dependent growth rate. Diatoms are distinguished from small phytoplankton by an additional nutrient dependence (silica) and a sinking rate of 0.5 m/day. Phytoplankton losses occur as a result of both zooplankton grazing and natural mortality. Zooplankton growth is a function of temperature and phytoplankton availability, with a preference for small phytoplankton. This

parameterization provides a direct bottom-up response of zooplankton to changes in phytoplankton population, but does not include complex processes such as vertical migration or omnivory [*Pangle and Peacor* 2010]. Organic matter generated as a result of phytoplankton and zooplankton mortality and sloppy grazing by zooplankton is remineralized back to inorganic matter at a constant rate. Carbon and phosphorus are traced based on a constant C:P molar ratio of 200, which is used to calculate phytoplankton and zooplankton biomass. This value is similar to those used by previous Great Lakes modeling studies [*Bennington et al.,* 2012; *White and Matsumoto* 2012; *Pilcher et al.,* 2015]. River tributary loads of phosphorus are not directly spatially resolved, as our goal is not to simulate the instantaneous response of these loads, but rather the lakewide long-term impact on the background phosphorus concentration, which is implemented by the model initial concentrations (section 2.4; Table 1). Additional model details can be found in the supplementary text [*Wanninkhof* 1992; *Lewis and Wallace* 1998; *Pilcher et al.,* 2015].

2.2 Quagga Mussel Forcing

Quagga mussels (*Dreissena rostriformis bugensis*) are added to the model as an additional phytoplankton loss term active only in the model vertical layer that is the lake bottom (Figure 2, dashed lines). With the inclusion of quagga mussel grazing, the time rate of change of phytoplankton becomes:

$$\frac{dPhy_i}{dt} = phy_i * \mu_{phy_i} - graz_{phy_i} * zoo * T_{func} - mort * phy_i - graz_{quagga} * phy_i \qquad (1)$$

where the first term represents phytoplankton growth, the second term is grazing of phytoplankton by zooplankton, the third term is phytoplankton mortality, and the fourth term is

grazing of phytoplankton by quagga mussels. The quagga mussel grazing term is calculated as a loss of phytoplankton biomass using the following equation:

$$graz_{quagga} = quagga\ density * filtration\ rate/z\_thickness \quad (2)$$

where *quagga density* is the density of quagga mussels (# of mussels/m^2), *filtration rate* is the mussel filtration rate (L/mussel/day), and *z_thickness* is the thickness of the model vertical layer (m). We use a constant filtration rate of 225 ml/mussel/hr (5.4 L/mussel/day), which is comparable to average rates for larger mussels reported by *Diggins* [2001] and *Baldwin et al.,* [2002]. Although *Diggins* [2001] report filtration rates that vary with temperature and mussel size, for this first implementation, we choose a simpler form without temperature and size dependency and note that this dependency is unlikely to significantly alter our model results (supplementary text S3).

To calculate the density of quagga mussels, we utilize data from *Nalepa et al.,* [2010] and *Nalepa et al.,* [2014], both of which provide observed quagga mussel densities at the following four depth intervals: < 30m, 31-50m, 51-90m, and > 90m. Using these data, a mussel population density is imposed in the bottom layer of the model based on the lake bathymetric depth and the corresponding depth interval value (Figure 3; supplementary text S2). We then linearly interpolate to daily resolution from 2007-2010 to avoid abrupt transitions between yearly changes in observed mussel population density. Mussels increase throughout the entire timeframe at all depths greater than 51m, consistent with the expansion of mussels offshore following nearshore establishment [*Nalepa et al.,* 2010]. Mussels between 31-50m already reached an upper limit by 2006-2007, and then declined by 33% for the lake-wide average by 2010. This dynamic is consistent with an introduced species initially overshooting its stable population level due to rapid growth and then declining towards a quasi-equilibrium based on

resource constraints [*Crooks* 2005]. The mussels may have also matured from a relatively smaller size, juvenile population to a larger sized adult population. This hypothesis is supported by the observation that although mussel density declined between 2005-2010, the mean biomass stayed the same [*Nalepa et al.,* 2014]. Mussels in the less than 30m depth range increase and decrease on a year-by-year basis, indicating no clear pattern. This depth range contains the most significant uncertainty in observed estimates [*Nalepa et al.,* 2010] and is likely impacted by substantial spatial heterogeneity.

2.3 Observational Data

For comparison to model output, we utilize phytoplankton count data from 2007-2010 collected at offshore locations as part of the EPA Great Lakes Monitoring Program (https://www.epa.gov/great-lakes-monitoring). These data are collected during "spring" (approximately April) and "summer" (approximately August) at 11 stations throughout Lake Michigan (Figure 1) and have been previously used to diagnose long-term phytoplankton trends [*Reavie et al.,* 2014]. Spring isothermal samples integrated equal volumes of water from 1, 5, 10, and 20m depth and summer stratified samples integrated equal volumes from 1m, 5m, and 10m, and the lower epilimnion. Phytoplankton count data are classified by taxa and are reported as cell density (cells/ml) and biovolume (μm^3/ml). Observed biovolume is converted to biomass (mgC/m^3) using the carbon-volume ratio of 0.20 ($pgC/\mu m^3$) calculated for freshwater algae by *Rocha and Duncan* [1985]. Because the model employs only two phytoplankton groups and thereby does not contain the taxonomic resolution of the observations, we focus on total phytoplankton as the metric for model validation. For the observations, this includes the sum total of all sampled phytoplankton, classified by *Reavie et al.,* [2014] as centric diatoms, pennate

diatoms, chlorophytes (green algae), chrysophytes, cryptophytes, cyanobacteria (blue-green algae), and pyrrophytes (dinoflagellates). We consider this to encompass the total biomass of photosynthetic plankton, which is most analogous to the sum of the two modeled phytoplankton groups, though picoplankton (< 2μm) are not included in the monitoring program. *Carrick et al.,* [2015] report a recent shift in phytoplankton composition towards picoplankton, which could lead to a low bias in the total observed phytoplankton biomass. Comparisons between total diatoms and non-diatoms are also provided in the supplementary information.

For additional model validation, we employ daily areal integrated primary production data from two offshore stations located in the southern basin of Lake Michigan (Figure 1). These data are reported in *Fahnenstiel et al.,* [2010] and are derived from observed photosynthetic rates obtained via the ^{14}C incubation method and incorporated into the Great Lakes Production Model [*Lang and Fahnenstiel* 1996]. Data are assumed to be gross primary production (GPP) due to the short (1-2 h) incubation time. The model estimates only net primary productivity (NPP). An average factor of 1.4 is used to convert between GPP and NPP based on the 40% average difference between GPP and NPP reported in *Fahnenstiel and Scavia* [1987]. However, the GPP to NPP ratio can vary between 1.18-1.84, with smaller values typically occurring during the spring bloom and larger values occurring during nutrient-limited periods [*Fahnenstiel and Scavia* 1987; *Pilcher et al.,* 2015]. Previous comparisons of this model to data of *Fahnenstiel et al.,* [2010] illustrate that the model falls in the upper range of observed productivity, but still within the range generated by the variable GPP to NPP ratio. Furthermore, the model spring bloom occurs a few weeks earlier than the observed bloom, due to an earlier termination of spring isothermal mixing resulting from an established model warm bias

[*Bennington et al.,* 2010; *Pilcher et al.,* 2015]. For a complete description and further model validation details please refer to the supplementary text and *Pilcher et al.,* [2015].

2.4 Model Scenarios

A total of 4 model scenario runs are presented here (Table 1). The goal of these scenarios is to separate the lakewide biogeochemical impacts due to quagga mussels from those due to the direct effects of lower total phosphorus concentrations. The former has a direct, top-down grazing impact on phytoplankton, while the later represents a bottom-up control on phytoplankton growth. The two effects generate a similar result (i.e. reduction of primary productivity) but through two different mechanisms. Thus, we run separate simulations to test each mechanism individually and also test the combined effect. This approach allows us to fully elucidate the lakewide response and its seasonal patterns. However, we note that the lakewide response is likely more representative of the offshore system because the model validation uses primarily offshore observational data and does not include spatially resolved nearshore nutrient inputs. The "Past Nutrients" scenario has neither quagga mussel grazing nor changed nutrient concentrations, and is therefore considered the "Control" simulation [*Pilcher et al.,* 2015, Table 1]. The "Present Nutrients" scenario models the impacts due to changing lakewide nutrient concentrations between the 1983-1999 pre-quagga and 2000-2008 post-quagga timeframes described by *Mida et al.,* [2010]. Although the decrease in total phosphorus over this timeframe is often connected to a decrease in phosphorus loading, it is likely that mussels have also impacted phosphorus concentrations, through benthic sequestration in shells, feces, and pseudofeces [*Bootsma et al.,* 2012; *Mosley and Bootsma* 2015]. Thus, the "Present Nutrients" simulation is not completely independent of quagga mussels. This would require a quantitative

lakewide estimate of the decrease attributable to mussels, which to our knowledge does not exist. The "Quagga Past Nutrients" scenario exclusively models the impact of quagga mussel grazing. The "Quagga Present Nutrients" scenario includes both effects and is most representative of the current lake system. Aside from these differences, all model simulations are identical and use the same atmospheric forcing from 2006-2010. Spatial maps comparing differences between the model scenarios depict values averaged over the top 25m.

3. Results

3.1 Model Validation

The model accurately captures the observed seasonal increase in total phytoplankton biomass between spring and summer, and is comparable in magnitude to the observed biomass in spring and summer (Figure 4). Model values never fall outside the observed variability, with average RMSE values of 3.2 and 8.1 mgC/m^3 for spring and summer respectively. Variability is generally greater in the observations compared to the model, though both show enhanced variability in the summer compared to the spring. Differences between station locations are also similar between the model and observations (supplementary figure S4), suggesting that the model is effective at reproducing broad patterns of spatial variability.

We also compare model GPP to observed GPP from *Fahnenstiel et al.,* [2010] for two timeframes. The first timeframe is representative of the pre-quagga lake, and compares the Past Nutrients model simulation to observed data collected prior to quagga mussel establishment (Figure 5a). The second timeframe is representative of the post-quagga lake, and compares the Quagga Present Nutrients simulation and observed data from 2007-2008 (Figure 5b). The model captures the general shape and magnitude of the seasonal cycle, with an annual RMSE of 259

and 249 mgC/m^2/day for the pre-quagga and post-quagga periods respectively. However, the model peak in GPP associated with the spring/summer phytoplankton bloom tends to occur 1-2 months earlier than the observed peak in both comparisons. This is consistent with an earlier onset of stratification due to a warm bias in the model NARR forcing [*Pilcher et al.,* 2015; *Rowe et al.,* 2015a]. This difference is most pronounced in May of the post-quagga timeframe (Figure 5b), when simulated and observed GPP are 218 and 851 mgC/m^2/day respectively. This disagreement is immediately balanced in June and July, when simulated GPP is less than observed GPP. The similar magnitude of peak GPP between the model and observations further suggests that the disagreement mainly results from an earlier spring bloom. This bias in the timing of the spring bloom can impact productivity by reducing the amount of time mussels can graze on phytoplankton and by increasing the amount of time phytoplankton spend in stratified, nutrient-limited conditions. The two processes have counteracting effects (i.e. increasing and decreasing productivity respectively), which may help explain the comparatively lower biases in summer productivity and phytoplankton biomass. Modeled zooplankton also likely peak too early in response to the earlier peak in productivity.

3.2 Separating Impact of Nutrients and Quagga Mussels

Spatial plots of 4-year annual mean NPP, phytoplankton, and zooplankton biomass averaged over the top 25m for the "Past Nutrients" simulation are shown in Figure 6. Maximum annual NPP occurs along the shoreline, particularly along the western shoreline, an area of frequent summer coastal upwelling [*Pilcher et al.,* 2015]. In general, NPP decreases when moving offshore and the southern basin contains greater overall rates compared to the northern basin. Offshore NPP is 75-100 mgC/m^2/day in the southern basin, and 50-75 mgC/m^2/day in the

deeper northern basin. Phytoplankton biomass displays a very similar spatial pattern to NPP, with maximum concentrations found in regions near the shoreline. Zooplankton biomass is greatest in nearshore regions, though the spatial pattern is somewhat different compared to NPP and phytoplankton biomass. For instance, zooplankton biomass is relatively high in Green Bay while productivity and phytoplankton biomass are relatively lower. This disconnect results from the shallower (<50m) depths within Green Bay that allow zooplankton to locate and graze on phytoplankton more effectively than at deeper, open-lake locations. Thus, in Green Bay and in shallower regions of northeast Lake Michigan, modeled zooplankton exert a relatively stronger top-down control on phytoplankton production.

Reducing total phosphorus concentrations to present day conditions ("Present Nutrients") produces a net decline in NPP, phytoplankton, and zooplankton (Figure 7a-c). Throughout most of the offshore lake, NPP declines by 20-30%, with localized nearshore declines of 30-40%. Net declines in total offshore phytoplankton range from 0-20%, with a region of 20-30% total decline along the western shoreline. The net change in zooplankton is relatively greater, with most regions declining by 30-40%.

The addition of quagga mussels alone ("Quagga Past Nutrients") produces a substantial net decline in nearshore NPP, phytoplankton, and zooplankton compared to the "Past Nutrients" simulation (Figure 7d-f). The net decline in all three parameters is substantially greater in magnitude and more spatially heterogeneous than the net declines due only to changing nutrient concentrations (Figure 7a-c). Net declines are strongly spatially correlated with lake depth (correlation values of 0.75, 0.83, and 0.78 for NPP, phytoplankton, and zooplankton, respectively) and decrease in magnitude from nearshore to offshore locations. Phytoplankton biomass actually increases in offshore regions of the northern basin by 0-20%.

The combined effect of both reduced nutrient concentrations and the addition of quagga mussels with the "Quagga Present Nutrients" simulation (Figure 7g-i) has a spatial pattern similar to the impact of exclusively adding quagga mussels ("Quagga Past Nutrients" simulation, Figure 7d-f), but with a greater magnitude, particularly in offshore regions. The offshore decline is greatest for NPP and zooplankton biomass.

Figure 8 displays 0-25m averaged NPP, phytoplankton, and zooplankton following both changes, i.e. in the "Quagga Present Nutrients" simulation. Comparison to "Past Nutrients" (Figure 6) illustrates the substantial impact to all three variables due to both processes. Whereas "Past Nutrients" displayed a decreasing nearshore-offshore gradient, "Quagga Present Nutrients" shows the reverse, with lakewide phytoplankton productivity now concentrated in offshore regions. The total magnitude of this offshore productivity is reduced in comparison to "Past Nutrients". Western nearshore NPP and phytoplankton biomass are still slightly enhanced, but not to the same extent as "Past Nutrients". Maximum phytoplankton and zooplankton biomass shift to the deeper central basins.

The separate and combined effects of changing nutrients and quagga mussels is further illustrated by comparing the seasonal rates of lakewide averaged NPP for all 4 simulations (Figure 9). Reduced nutrient concentrations lower NPP from January-May, but the quagga mussels have a much greater effect overall. The presence of quagga mussels actually negates the effect of nutrients while the lake is unstratified from January through mid-April, as evidenced by the nearly identical rates of NPP between the "Quagga Past Nutrients" and "Quagga Present Nutrients" simulations. Once the lake begins to stratify in mid-April, NPP in both quagga mussel simulations rapidly increases to the peak levels simulated in the respective no quagga scenarios with the same nutrient concentrations. After the spring bloom, NPP declines and

stabilizes at a relatively constant summer value, before declining in winter. While the lake is stratified from June-September, NPP is largely independent of quagga mussels and is instead dependent on nutrient concentrations. Conversely, November-December NPP is again dominated by the presence of quagga mussels. Figure 9 illustrates that from a lakewide perspective, November-April NPP is strongly impacted by quagga mussels, whereas June-September NPP is strongly impacted by nutrient concentrations. Furthermore, reduced nutrients retain the same seasonal cycle but with lower overall productivity, while quagga mussels alter the seasonal cycle but retain similar levels of summer productivity. Inclusion of both processes produces the best comparison to observed offshore GPP rates, though the inclusion of quagga mussels is the more critical process (supplementary figure S5).

4. Discussion

In this model, unstratified late winter-spring (January-May) productivity is substantially reduced by the addition of quagga mussels. This reduction results from isothermal mixing of phytoplankton to the bottom layer where quagga mussels efficiently consume them. Lake vertical mixing is sufficient to support this mechanism, even at locations with depths greater than 90 m (Figure 5b). This process can also be examined using the critical depth hypothesis, which has been invoked in previous Lake Michigan studies to explain the timing of the spring bloom [*Sverdrup* 1953; *Pilcher et al.,* 2015; *Rowe et al.,* 2015b]. Mussel grazing acts as an additional phytoplankton loss term, which delays the timing of when the mixed layer depth (MLD) shallows to the critical depth that allows for net phytoplankton growth. An increase in MLD due to mussel grazing would also produce a similar effect, however, model MLDs already encompass nearly the entire water column in the pre-quagga scenarios (figure not shown). Thus,

MLDs are relatively unchanged with the inclusion of quagga mussels. Conversely, the euphotic depth of some offshore regions increases by ~ 5m with the inclusion of quaggas, which would lend to an increase in productivity due to a deepening of the critical depth. Yet, these offshore regions still display a net decrease in productivity, suggesting that quagga mussel grazing is the dominant process.

Thermal stratification eliminates the loss process due to mussels, enabling June-September productivity to rebound to pre-quagga levels. Modeled phytoplankton during stratification remain in the epilimnion, which protects them from benthic quagga mussel grazing. Productivity is then eventually limited by depleted epilimnetic nutrient concentrations and zooplankton grazing, as in the pre-quagga model [*Pilcher et al.,* 2015]. This seasonal dependence of quagga mussel grazing is consistent with studies citing quagga mussels as the primary mechanism for the observed Lake Michigan productivity changes [*Fahnenstiel et al.,* 2010; *Kerfoot et al.,* 2010; *Vanderploeg et al.,* 2010; *Rowe et al.,* 2015a]. Nearshore regions (< 20m) are an exception to this seasonal dependency, since maximum depths are shallower than the surface mixed layer, resulting in year-round grazing by mussels. Thus, reductions in NPP, phytoplankton, and zooplankton biomass are substantially greater in the nearshore compared to the offshore, producing a sign reversal in the nearshore-offshore gradient between the pre-quagga and post-quagga lake (i.e. greatest productivity located nearshore in pre-quagga lake but offshore in post-quagga lake). This result has also been observed using satellite remote sensing data [*Fahnenstiel et al.,* 2016].

Cumulative lakewide NPP is reduced from 8.5 TgC/year in the "Past Nutrients" simulation, to 4.7 TgC/year after the addition of quagga mussels and lower nutrients ("Quagga Present Nutrients"). These values are lower than the 2008 value of 9.5 TgC/year estimated by

Warner and Lesht [2015], but close to the 5.0-7.2 TgC/year estimate by *Fahnenstiel et al.,* [2016] for 2010-2013. Using a 1.4 NPP:GPP conversion factor [*Pilcher et al.,* 2015; *Fahnenstiel and Scavia* 1987] yields a model GPP estimate of 6.6 TgC/year, which falls within the range of *Fahnenstiel et al.,* [2016]. This may be the more appropriate comparison, because the method and short incubation time used by *Fahnenstiel et al.,* [2016] is similar to that used by *Fahnenstiel et al.,* [2010] for model validation. The variance in these estimates illustrates the substantial uncertainty in estimating total lakewide productivity, even when using similar methods. Both *Warner and Lesht* [2015] and *Fahnenstiel et al.,* [2016] utilize satellite-derived input parameters and a productivity model to arrive at their estimates. However, *Fahnenstiel et al.,* [2016] suggest that the *Warner and Lesht* [2015] values may be biased high, in part, due to the use of ocean-based satellite retrieval parameters, rather than parameters specific to the Great Lakes. Further differences in spatial and temporal scale, and the handling of winter productivity are also listed as possible explanations for the difference. Overall, our model value is within the range of uncertainty presented by previous satellite-derived estimates but falls closer to *Fahnenstiel et al.,* [2016].

The impact of this loss of lakewide NPP on the inorganic carbon cycle has received relatively little attention in the literature. Previous modeling work showed that the seasonal carbon cycle is defined by biological processes driving net carbon uptake from March-June and physical processes (e.g. temperature and vertical mixing) driving net carbon efflux to the atmosphere from July-February [*Pilcher et al.,* 2015]. Thus, we may expect reduced carbon uptake in the post-quagga lake due to the reduction in NPP. Figure 10 illustrates that a reduced spring bloom does lead to substantially higher values of March-May surface pCO_2. However, this result also produces interesting downstream effects due to the interaction of this biologically

driven change with the underlying lake physical processes. For example, offshore fall-winter pCO_2 is lower in the post-quagga lake, which does not appear consistent with reduced productivity. This feature can be explained by considering the deep vertical mixing that brings up remineralized carbon that previously sank below the mixed layer, elevating pCO_2 values [*Pilcher et al.,* 2015]. Reduced March-June productivity decreases this export of organic carbon, resulting in a decreased return flux in fall-winter. Lakewide surface pCO_2 is also lower during the stratified timeframes (Figure 10e), which is the opposite of what might be expected with reduced productivity in the post-quagga lake (Figure 9). The cause is a substantially reduced period of lake carbon uptake (2 months vs. 5 months in the respective post-quagga and pre-quagga lake), which reduces July-August epilimnion concentrations of dissolved inorganic carbon (DIC; figure not shown). This contributes to an overall dampening of the seasonal cycle. These model results are difficult to verify due to the lack of inorganic carbon chemistry data. Additional mussel processes not included in our model implementation, such as a reduction in total alkalinity due to increased mussel calcification [*Barbiero et al.,* 2006], may also be necessary to fully assess the lakewide carbon cycle response to quagga mussels.

There is concern that the substantial reduction in primary productivity will have cascading effects to higher trophic levels. In recent years, populations of zooplankton and native benthic inverterbrates (e.g. *Diporeia*) have significantly declined [*Bunnell et al.,* 2014], forcing some fish to graze on *Dreissena* mussels that are much lower in energy content [*Nalepa et al.,* 2009]. Commercially important fish may be unable to increase predation to the extent required to make up this energy deficit, resulting in lower growth rates and fish weight [*Pothoven and Madenjian* 2008]. Our model results suggest a 52% decline in annual mean lakewide zooplankton population when accounting for quagga mussels and lower nutrient concentrations.

This decline is consistent with observed total zooplankton biomass declines of 25-57% in nearshore to offshore sample locations when comparing the 1970s to 2007-2012 [*Pothoven and Fahnenstiel* 2015]. Recent isotope analysis suggests that pelagic fish have become less reliant on offshore food sources and more reliant on nearshore benthic algal subsidies [*Turschak et al.,* 2014]. Though our model does not explicitly represent benthic productivity and its changes due to quagga mussels, the decline in pelagic food sources indicated by *Turschak et al.,* [2014] does agree with our modeled zooplankton decline in offshore regions.

These results are potentially sensitive to key parameters and features of the model. For example, the C:P ratio has a large impact on lakewide productivity and phytoplankton biomass. Sensitivity tests indicate that modeled NPP is more sensitive to the C:P ratio of diatoms than to the C:P of small phytoplankton (supplementary text S4; *Hecky et al.,* 1993; *Elser et al.,* 2000; *Sterner et al.,* 2008; *Hessen et al.,* 2012). Our selected C:P value of 200 is a reasonable estimate for the lakewide mean, though significant deviations from this value are observed [*Bootsma et al.,* 2012]. However, without a mechanistic explanation for this observed variance, a constant value is a necessary simplification.

Spatially, the reduction in productivity is strongly correlated with depth, which also suggests a strong correlation with mussel population density. Therefore, spatial heterogeneity in mussel density populations may propagate to phytoplankton and zooplankton biomass. The impact of mussel density variations are tested based on the distributions across the years 2008-2010 and across depth ranges (Figure S1, Supplementary text). Greater sensitivity is found to lake depth than to mussel population density, with density having a <10% impact on NPP changes.

Lastly, the spatial patterns of change found here could be impacted by the exclusion of spatially resolved phosphorus river loading. In fact, modeled mussel grazing is sufficient to suppress phytoplankton populations in nearshore (≤ 20m) locations year-round despite the fact that there is always available phosphorus (supplementary figure S6). Thus, local phosphorus inputs from rivers are unlikely to support additional net phytoplankton productivity in the nearshore. Given offshore nutrient limitation during the stratified summertime, it is possible that export of river plumes to the offshore could boost offshore summer productivity. However, nearshore sequestration by mussels may prevent this offshore transport, thereby exacerbating *Cladophora* blooms, with little net effect to offshore productivity.

Our results suggest that both quagga mussels and changing nutrient concentrations are necessary to reproduce observed declines in Lake Michigan productivity from the mid-1980s to 2010. This result agrees with a recent modeling study which incorporated quagga mussel grazing to produce a decline in spring chlorophyll, but was unable to reproduce observed reductions summer chlorophyll without nutrient reductions [*Rowe et al.,* 2015a]. Satellite measurements also suggest quagga grazing is the dominant control on spring productivity, but phosphorus loading and climate variability are dominant controls on summer productivity in Lake Michigan [*Warner and Lesht* 2015]. A food-web model study in Saginaw Bay, Lake Huron found a similar sensitivity to both phosphorus inputs and *Dreissena* grazing, with the most significant *Dreissena* impacts occurring at much lower phosphorus concentrations [*Yu-Chun et al.,* 2014]. These authors suggest that because of *Dreissena* mussels, target nutrient limits may need to be reconsidered and potentially relaxed in order to avoid deleterious impacts to upper-trophic organisms. However, mechanisms that couple phosphorus cycling and quagga mussels may further complicate the response. For example, quagga mussels can sequester riverine inputs

of phosphorus in the nearshore and transfer phosphorus from the water column to the benthos [*Hecky et al.,* 2004; *Mosley and Bootsma* 2015]. This "nearshore phosphorus shunt" promotes the growth of nearshore nuisance *Cladophora* while decreasing offshore phosphorus concentrations [*Bootsma et al.,* 2012]. Coupled interactions between phosphorus loading, quagga mussels, and *Cladophora* are currently not represented in models (including MITgcm.Michigan), but are likely necessary to gain a complete understanding of nearshore/offshore dynamics and the effect of phosphorus loading limits [*Bootsma et al.,* 2015].

Acknowledgments

The authors thank the UW Madison-Milwaukee Intercampus Grant Program, NASA (NNX/11AD59G), the UW-Madison's Climate People and the Environmental Program at the Center for Climatic Research, and the Wisconsin Space Grant Consortium for funding this project. Part of this project was also completed while D.J.P. held a National Research Council Research Associateship award at the Pacific Marine Environmental Laboratory. All model analysis was performed using the MITgcm, which is freely available from http://mitgcm.org. Necessary code modifications required to configure MITgcm to Lake Michigan and incorporate quagga mussels, along with the computation scripts used to generate the manuscript figures can be found at https://github.com/darren-pilcher/MITgcm-Michigan. NARR Reanalysis data was obtained from the NOAA/OAR/ERSL PSD, Boulder, Colorado, USA, from the website http://www.esrl.noaa.gov/psd. Haidi Chen from the University of Wisconsin-Madison provided lake ice forcing from the U.S. National Ice Center. Comments from two reviewers greatly improved the manuscript. We also thank Samantha Siedlecki for reading an earlier draft of this manuscript and providing helpful feedback. This is PMEL contribution number 4523.

References

Baldwin, B.S., M.S. Mayer, J. Dayton, N. Pau, J. Mendilla, M. Sullivan, A. Moore, A. Ma, and E.L. Mills (2002), Comparative growth and feeding in zebra and quagga mussels (*Dreissena polymorpha* and *Dreissena bugensis*); implications for North American lakes, *Can. J. Fish. Aquat. Sci., 59*, 680-694, doi:10.1139/F02-043.

Barbiero, R.P., M.L. Tuchman, G.J. Warren, and D.C. Rockwell (2002), Evidence of recovery from phosphorus enrichment in Lake Michigan, *Can. J. Fish. Aquat. Sci., 59*, 1639-1647, doi:10.1139/F02-132.

Barbiero, R.P., M.L. Tuchman, and E.S. Millard (2006), Post-dreissenid Increases in Transparency During Summer Stratification in the Offshore Waters of Lake Ontario: Is a Reduction in Whiting Events the Cause?, *J. Great Lakes Res., 32,* 131-141, doi:10.3394/0380-1330(2006)32[131:PIITDS]2.0.CO;2.

Bennington V., G.A. McKinley, N. Kimura, and C.H. Wu (2010), General circulation of Lake Superior: Mean, variability, and trends from 1979 to 2006, *J Geophys. Res., 115,* C12015, doi:10.1029/2010JC006261.

Bennington, V., G.A. McKinley, N. Urban, and C. McDonald (2012), Can spatial heterogeneity explain the perceived imbalance in Lake Superior's carbon budget? A model study, *J. Geophys. Res., 117*, G03020, doi:10.1029/2011JG001895.

Bootsma, H.A. and R.E. Hecky (2003), A Comparative Introduction to the Biology and Limnology of the African Great Lakes, *J. Great Lakes Res., 29*(2), 3-18, doi: 10.1016/S0380-1330(03)70535-8.

Bootsma, H.A., J.T. Waples, and Q. Liao (2012), Identifying Major Phosphorus Pathways in the Lake Michigan Nearshore Zone, MMSD Contract M03029P05, Milwaukee Metropolitan Sewerage District, Milwaukee, WI.

Bootsma, H.A., M.D. Rowe, C.N. Brooks, and H.A. Vanderploeg (2015), Commentary: The need for model development related to *Cladophora* and nutrient management in Lake Michigan, *J. Great Lakes Res., 41*, doi:10.1016/j.jglr.2015.03.023.

Bunnell, D.B., R.P., Barbiero, S.A. Ludsin, C.P. Madenjian, G.J. Warren, D.M. Dolan, T.O. Brenden, R. Briland, O.T. Gorman, J.X. He, T.H. Johengen, B.F. Lantry, B.M. Lesht, T.F. Nalepa, S.C. Riley, C.M. Riseng, T.J. Treska, I. Tsehaye, M.G. Walsh, D.M. Warner, and B.C. Weidel (2014), Changing Ecosystem Dynamics in the Laurentian Great Lakes: Bottom-Up and Top-Down Regulation, *Bioscience, 64*, 26-39, doi:10.1093/biosci/bit001.

Carrick, H.J., E. Butts, D. Daniels, M. Fehringer, C. Frazier, G.L. Fahnenstiel, S. Pothoven, and H.A. Vanderploeg (2015), Variation in the abundance of pico, nano, and microplankton in Lake Michigan: Historic and basin-wide comparisons, *J. Great Lakes Res., 41,* doi:10.1016/j.jglr.2015.09.009.

Crooks, J.A. (2005), Lag times and exotic species: The ecology and management of biological invasions in slow-motion, *Ecoscience, 12*(3), 316-329, doi: 10.2980/i1195-6860-12-3-316.1.

Cuhel, R.L., and C. Aguilar (2013), Ecological Transformations of the Laurentian Great Lake Michigan by Nonindigenous Biological Invaders, *Annu. Rev. Mar. Sci.,* 5, 289-320, doi:10.1146/annurev-marine-120710-100952.

Diggins, T.P. (2001), A Seasonal Comparison of Suspended Sediment Filtration by Quagga (*Dreissena bugensis*) and Zebra (*D. polymorpha*) Mussels, *J. Great Lakes Res., 27*(4), 457-466.

Elser, J.J., W.F. Fagan, R.F. Denno, D.R. Dobberfuhl, A. Folarin, A. Huberty, S. Interlandi, S.S. Kilham, E. McCauley, K.L. Schulz, E.H. Siemann, and R.W. Sterner (2000), Nutritional constraints in terrestrial and freshwater food webs, *Nature, 408*, 578-580, doi: 10.1038/35046058.

Evans, M.A., G. Fahnenstiel, and D. Scavia (2011), Incidental Oligotrophication of North American Great Lakes, *Environ. Sci. Technol., 45*(8), 3297-3303, doi:10.1021/es103892w.

Fahnenstiel, G., and D. Scavia (1987), Dynamics of Lake Michigan Phytoplankton: Primary Production and Growth, *Can. J. Fish. Aquat. Sci., 44*, 499-508.

Fahnenstiel, G.L., G.A. Land, T.F. Nalepa, and T.H. Johengen (1995), Effects of Zebra Mussel (*Dreissena polymorpha*) Colonization on Water Quality Parameters in Saginaw Bay, Lake Huron, *J. Great Lakes Res., 21*(4), 435-448.

Fahnenstiel, G., S. Pothoven, H. Vanderploeg, D. Klarer, T. Nalepa, and D. Scavia (2010), Recent changes in primary Production and phytoplankton in the offshore region of southeastern Lake Michigan, *J. Great Lakes Res., 36*(supplement 3), 20-29.

Fahnenstiel, G.L., M.J. Sayers, R.A. Shuchman, F. Yousef, and S.A. Pothoven (2016), Lake-wide phytoplankton production and abundance in the Upper Great Lakes: 2010-2013, *J. Great Lakes Res., 42*(3), 619-629, doi:10.1016/j.jglr.2016.02.004.

Hecky, R.E., P. Campbell, and L.L. Hendzel (1993), The stoichiometry of carbon, nitrogen, and phosphorus in particulare matter of lakes and oceans, *Limnol. Oceanogr. 38*(4), 709-724, doi:10.4319/lo.1993.38.4.0709.

Hecky, R.E., R.E.H. Smith, D.R. Barton, S.J. Guildford, W.D. Taylor, M.N. Charlton, and T. Howell (2004), The nearshore phosphorus shunt: a consequence of ecosystem engineering by dreissenids in the Laurentian Great Lakes, *Can. J. Fish. Aquat. Sci., 61*, 1285-1293, doi:10.1139/F04-065.

Hessen, D.O., J.J. Elser, R.W. Sterner, and J. Urabe (2013), Ecological stoichiometry: An elementary approach using basic principles, *Limnol. Oceanogr., 58*(6), 2219-2236, doi: 10.4319/lo.2013.58.6.2219.

Johengen, T.H., O.E. Johannsson, G. Laird Pernie, and E.S. Millard (1994), Temporal and Seasonal Trends in Nutrient Dynamics and Biomass Measures in Lakes Michigan and Ontario in Response to Phosphorus Control, *Can. J. Fish. Aquat. Sci., 51*, 2570-2578.

Kerfoot, W.C., F. Yousef, S.A. Green, J.W. Budd, D.J. Schwab, and H.A. Vanderploeg, (2010), Approaching storm: Disappearing winter bloom in Lake Michigan, *J. Great Lakes Res., 36*, 30-41, doi:10.1016/j.jglr.2010.04.010.

Lang, G.A., and G.L. Fahnenstiel (1996), Great Lakes primary production model-methodology and use, NOAA Technical Memorandum ERL GLERL-90.

Lewis, E., and D.W.R. Wallace (1998), Program developed for CO2 system calculations, Rep. 105, 33 pp., Oak Ridge Natl. Lab., Oak Ridge, Tenn. [Available at http://cdiac.esd.ornl.gov/oceans/co2rprt.html].

Madenjian, C.P., D.B. Bunnell, D.M. Warner, S.A. Pothoven, G.L. Fahnenstiel, T.F. Nalepa, H.A. Vanderploeg, I. Tsehaye, R.M. Claramunt, and R.D. Clark Jr. (2015), Changes in the Lake Michigan food web following dreissenid mussel invasions: A synthesis, *J. Great Lakes Res., 41*(supplement 3), 217-231, doi:10.1016/j.jglr.2015.08.009.

Mason, L.A., C.M. Riseng, A.D. Gronewold, E.S. Rutherford, J. Wang, A. Clites, S.D.P. Smith, and P.B. McIntyre (2016), Fine-scale spatial variation in ice cover and surface temperature trends across the surface of the Laurentian Great Lakes, *Climatic Change, 138,* 71-83, doi:10.1007/s10584-016-1721-2.

Mesinger F., G. DiMego, E. Kalnay, K. Mitchell, P.C. Shafran, W. Ebisuzaki, D. Jovic, J. Woollen, E. Rogers, E.H. Berbery, M.B. Ek, Y. Fan, R. Grumbine, W. Higgins, H. Li, Y. Lin, G. Manikin, D. Parrish, and W. Shi (2006), North American regional reanalysis, *Bull. Am. Meteorol. Soc., 87*(3), 343–360, doi:10.1175/BAMS-87-3-343.

Michalak, A.M., et al. (2013), Record-setting algal bloom in Lake Erie caused by agricultural and meteorological trends consistent with expected future conditions, *Proc. Natl. Acad. Sci. U.S.A., 110*(16), 6448-6452, doi:10.1073/pnas.1216006110.

Mida, J.L., D. Scavia, G.L. Fahnenstiel, S.A. Pothoven, H.A. Vanderploeg, and D.M. Dolan (2010), Long-term and recent changes in southern Lake Michigan water quality with implications for present trophic status, *J. Great Lakes Res., 36*, 42-49.

Mosley, C. and H. Bootsma (2015), Phosphorus recycling by profunda quagga mussels (*Dreissena rostriformis bugensis*) in Lake Michigan, *J. Great Lakes Res., 41*(3), 38-48, doi:10.1016/j.jglr.2015.07.007.

Nalepa, T.F., D.J. Hartson, D.L. Fanslow, G.A. Lang, and S.J. Lozano (1998), Declines in benthic macroinvertebrate populations in southern Lake Michigan, 1980-1993, *Can. J. Fish. Aquat. Sci., 55*, 2402-2413.

Nalepa, T.F., D.L. Fanslow, and G.A. Lang (2009), Transformation of the offshore benthic community in Lake Michigan: recent shift from the native amphipod *Diporeia* spp. To the invasive mussel *Dreissena rostriformis bugensis*, *Freshwater Biology, 54*, 466-479, doi:10.1111/j.1365-2427.2008.02123.x.

Nalepa, T.F., D.L. Fanslow, and S.A. Pothoven (2010), Recent changes in density, biomass, recruitment, size structure, and nutritional state of *Dreissena* populations in southern Lake Michigan, *J. Great Lakes Res., 36*(supplement 3), 5-19.

Nalepa, T.F., D.L. Fanslow, G.A. Lang, K. Mabrey, and M. Rowe (2014), Lake-wide benthic surveys in Lake Michigan in 1994-95, 2000, 2005, and 2010: Abundances of the amphipod *Diporeia spp*. and abundances and biomass of the mussels *Dreissena polymorpha* and *Dreissena rostriformis bugensis*, NOAA Technical Memorandum GLERL-164, NOAA, Great Lakes Environmental Research Laboratory, Ann Arbor, MI 21 pp.

Nicholls, K.H., and G.J. Hopkins (1993), Recent Changes in Lake Erie (North Shore) Phytoplankton: Cumulative Impacts of Phosphorus Loading Reductions and the Zebra Mussel Introduction, *J. Great Lakes Res., 19*(4), 637-647.

Pangle, K.L., and S.D. Peacor (2010), Temperature gradients, not food resource gradients, affect growth rate of migrating *Daphnia mendotae* in Lake Michigan, *J. Great Lakes Res., 36(2)*, 345-350, doi:10.1016/j.jglr.2010.01.005.

Phillips, J.C., G.A. McKinley, V. Bennington, H.A. Bootsma, D.J. Pilcher, R.W. Sterner, and N.R. Urban (2015), The potential for CO_2-induced acidification in freshwater: a Great Lakes case study, *Oceanography 28*(2), 136-145, doi:10.5670/oceanog.2015.37.

Pilcher, D.J., G.A. McKinley, V. Bennington, and H. Bootsma (2015), Physical and biogeochemical mechanisms of internal carbon cycling in Lake Michigan, *J. Geophys. Res. Oceans, 120*(3), 2112-2128, doi:10.1002/2014JC010594.

Pothoven, S.A., and C.P. Madenjian (2008), Changes in Consumption by Alewives and Lake Whitefish after Dreissenid Mussel Invasions in Lakes Michigan and Huron, *N. Am. J. Fish. Manage., 28*:1, 308-320, doi:10.1577/M07-022.1.

Pothoven, S.A., and G.L. Fahnenstiel (2015), Spatial and temporal trends in zooplankton assemblages along a nearshore to offshore transect in southeastern Lake Michigan from 2007 to 2012, *J. Great Lakes Res., 41*, 95-103, doi:10.1016/j.jglr.2014.09.015.

Reavie, E.D., R.P. Barbiero, L.E. Allinger, and G.J. Warren (2014), Phytoplankton trends in the Great Lakes, 2001-2011, *J. Great Lakes Res., 40*, 618-639.

Rocha, D., and A. Duncan (1985), The Relationship between Cell Carbon and Cell-Volume in Fresh-Water Algal Species Used in Zooplanktonic Studies*, J. Plankton Res., 7*(2), 279-294.

Rothlisberger, J.D., D.C. Finnoff, R.M. Cooke, and D.M. Lodge (2012), Ship-borne Nonindigenous Species Diminish Great Lakes Ecosystem Services, *Ecosystems 15*, 462-476, doi:10.1007/s10021-012-9522-6.

Rowe, M.D., E.J. Anderson, J. Wang, and H.A. Vanderploeg (2015a), Modeling the effect of invasive quagga mussels on the spring phytoplankton bloom in Lake Michigan, *J. Great Lakes Res., 41*(supplement 3), 49-65, doi:10.1016/j.jglr.2014.12.018.

Rowe, M.D., D.R. Obenour, T.F. Nalepa, H.A. Vanderploeg, F. Yousef, and W.C. Kerfoot (2015b), Mapping the spatial distribution of the biomass and filter-feeding effect of invasive dreissenid mussels on the winter-spring phytoplankton bloom in Lake Michigan, *Freshwater Biol., 60,* 11, 2270-2285, doi:10.1111/fwb.12653.

Smith, S.D.P., et al. (2015), Rating impacts in a multi-stressor world: a quantitative assessment of 50 stressors affecting the Great Lakes, *Ecological Applications, 25*(3), 717-728, doi:10.1890/14-0366.1.

Sterner, R.W., T. Anderson, J.J. Elser, D.O. Hessen, J.M. Hood, E. McCauley, and J. Urabe (2008), Scale-dependent carbon : nitrogen : phosphorus seston stoichiometry in marine and freshwaters, *Limnol. Oceanogr., 53*(3), 1-13, doi: 10.2307/40058228.

Stow, C.A. (2015), The need for sustained, long-term phosphorus modeling in the Great Lakes, *J. Great Lakes Res., 41*(2), 315-316, doi:10.1016/j.jglr.2015.03.001.

Sverdrup, H.U. (1953), On conditions for the vernal blooming of phytoplankton, *J. Cons. Cons. Int. Explor. Mer, 18*, 287-295.

Turschak, B.A., D. Bunnell, S. Czesny, T.O. Höök, J. Janssen, D. Warner, and H.A. Bootsma (2014), Nearshore energy subsidies support Lake Michigan fishes and invertebrates following major changes in food web structure, *Ecology, 95*(5), 1243-1252, doi:10.1890/13-0329.1.

U.S. National Ice Center (2010), Great Lakes Ice Analysis Products, U.S. National Ice Center Naval Ice Center, Aug 15 2011.

Vanderploeg, H.A., J.R. Liebig, T.F. Nalepa, G.L. Fahnenstiel, and S.A. Pothoven (2010), *Dreissena* and the disappearance of the spring phytoplankton bloom in Lake Michigan, *J. Great Lakes Res., 36*, 50-59, doi:10.1016/j.jglr.2010.04.005.

Waples, J.T., H.A. Bootsma, and J.V. Klump (2017), How are coastal benthos fed?, *Limnol. Oceanogr. 2,* 18-28, doi:10.1002/lol2.10033.

Wanninkhof, R. (1992), Relationship between wind speed and gas exchange over the ocean, *J.*

Geophys. Res., 97(C5), 7373–7382, doi:10.1029/92JC00188.

Warner, D.M., and B.M. Lesht (2015), Relative importance of phosphorus, invasive mussels and climate for patterns in chlorophyll a and primary production in Lakes Michigan and Huron, *Freshwater Biology, 60*, 1029-1043, doi:10.1111/fwb.12569.

White, B. and K. Matsumoto (2012), Causal mechanisms of the deep chlorophyll maximum in Lake Superior: A numerical modeling investigation, *J. Great Lakes Res., 38*(3), 504-513, doi: 10.1016/j.jglr.2012.05.001.

Yu-Chun, K., S. Adlerstein, and E. Rutherford (2014), The relative impacts of nutrient loads and invasive species on a Great Lakes food web: An Ecopath with Ecosim analysis, *J. Great Lakes Res., 40*, 35-52, doi:10.1016/j.jglr.2014.01.010.

Table 1: Model Simulation Setup

	Model Scenario Name			
Variable	**Past Nutrients[a]**	**Present Nutrients**	**Quagga Past Nutrients**	**Quagga Present Nutrients**
Quagga Mussels	No	No	Yes	Yes
Total Phosphorus (µg/L)	6.8[b]	3.0[b]	6.8[b]	3.0[b]
Total Silicon (mg/L)	0.70[b]	0.80[b]	0.70[b]	0.80[b]

[a] This model version and results are described fully in *Pilcher et al.,* [2015].

[b] Nutrient initial conditions from *Mida et al.,* [2010].

Figure Captions

Figure 1: Map of Lake Michigan with observational locations used for model validation. The circles are the 11 stations used as part of the EPA Great Lakes Monitoring Program. The two starts labeled FA1 and FA2 are the two locations from *Fahnenstiel et al.,* [2010]. The contours are lake depth at 50m intervals.

Figure 2: Schematic illustration of the NPZD model modified from *Bennington et al.,* [2012]. Solid line arrows represent material flows between the different stocks. The dashed lines indicate the material flow due to quagga mussel grazing.

Figure 3: Annual average mussel population density for each year, mapped at four depth intervals: < 30m, 31-50m, 51-90m, and > 90m.

Figure 4: Spring (a) and summer (b) total phytoplankton biomass comparisons between the observations from the EPA Great Lakes Monitoring Program and the equivalent model locations. Shown is the average value across all 11 stations. The error bars signify the standard deviation across the stations.

Figure 5: Comparison of model and observed depth integrated GPP for the pre-quagga (a) and post-quagga (b) timeframes. Model values come from the Past Nutrients and Quagga Present Nutrients simulations respectively, and are averaged over the 2007-2008 forcing period. Observed values are from *Fahnenstiel et al.,* [2010]. Error bars are the standard deviation over the timeframe.

Note that there are no observed estimates for January and February.

Figure 6: 2007-2010 annual mean model values of (a) NPP, (b) total phytoplankton (i.e. combined small phytoplankton and diatoms), and (c) zooplankton for the Past Nutrients (i.e. control) simulation, averaged over the top 25m.

Figure 7: Difference plots of 0-25m averaged NPP, total phytoplankton, and zooplankton between the "Past Nutrients" (i.e. control) and the (a-c) "Present Nutrients", (d-f) "Quagga Past Nutrients", and (g-i) "Quagga Present Nutrients simulations. All values are plotted as a percent change compared to the "Past Nutrients" simulation. Negative values indicate a net decrease compared to "Past Nutrients". Contours are denoted at 10% intervals. Shown is the change in the annual mean over the entire 2007-2010 timeframe.

Figure 8: Average 0-25m values of NPP, total phytoplankton (i.e. combined PHY1 and PHY2), and zooplankton for the (a-c) "Past Nutrients" and for the (d-f) "Quagga Present Nutrients" simulation. Shown is the annual mean over the entire 2007-2010 timeframe.

Figure 9: (a) Lakewide averaged annual depth-integrated NPP for each simulation over the 2007-2010 timeframe. (b) Lakewide averaged surface water temperature and bottom water temperature for the "Past Nutrients" simulation, averaged over the 2007-2010 timeframe. Timeframes when the surface temperature is approximately equal to the bottom temperature are indicative of isothermal mixing.

Figure 10: (a-d) Spatial plots of the difference in partial pressure of CO_2 in surface water (pCO_2') for the "Quagga Present Nutrients" simulation compared to the "Past Nutrients" simulation. Positive anomaly values indicate an increase in pCO_2 for the "Quagga Present Nutrients" compared to the "Past Nutrients". The full field for "Past Nutrients" is shown in Pilcher et al. [2015]. (e) Lakewide averaged surface pCO_2 for the two simulations. The dashed line signifies the constant model atmospheric pCO_2 value of 385 µatm. Above the dashed line represents pCO_2 *supersaturation* and net carbon flux from the lake to the atmosphere. Below the dashed line represents pCO_2 *undersaturation* and net carbon flux from the atmosphere to the lake.

Figure 1

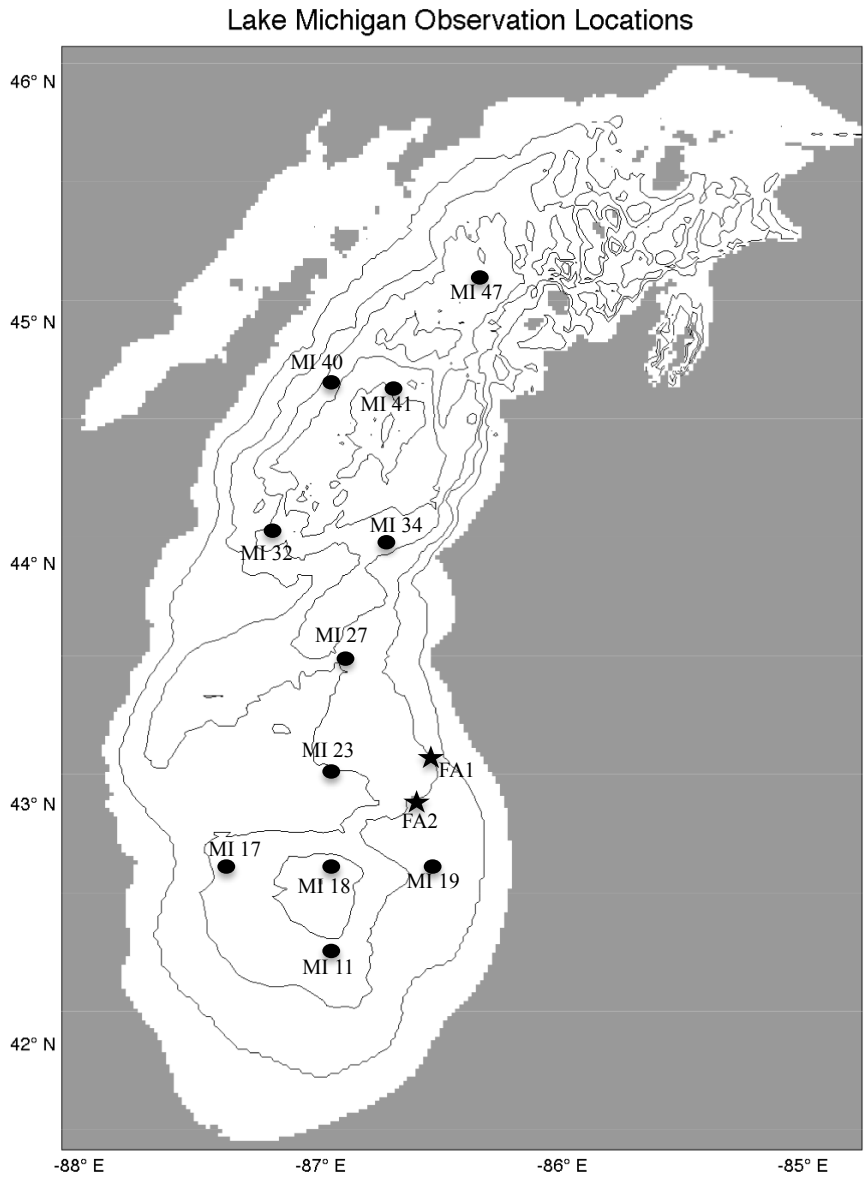
Lake Michigan Observation Locations
46° N
45° N
44° N
43° N
42° N
-88° E
-87° E
-86° E
-85° E
MI 47
MI 40
MI 41
MI 34
MI 32
MI 27
MI 23
FA1
FA2
MI 17
MI 18
MI 19
MI 11

Figure 2

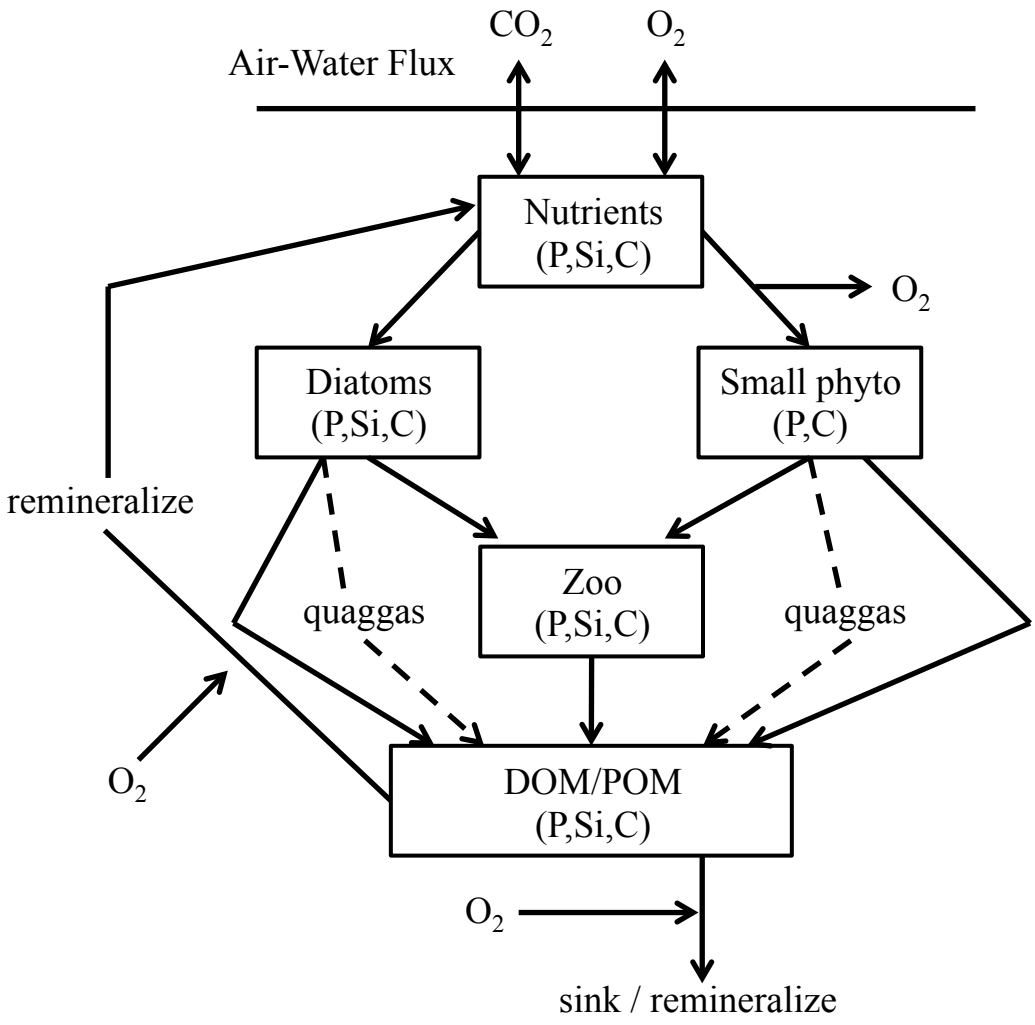
CO2
O2
Air-Water Flux
Nutrients
(P,Si,C)
O2
Diatoms
(P,Si,C)
Small phyto
(P,C)
remineralize
quaggas
Zoo
(P,Si,C)
quaggas
O2
DOM/POM
(P,Si,C)
O2
sink / remineralize

Figure 3

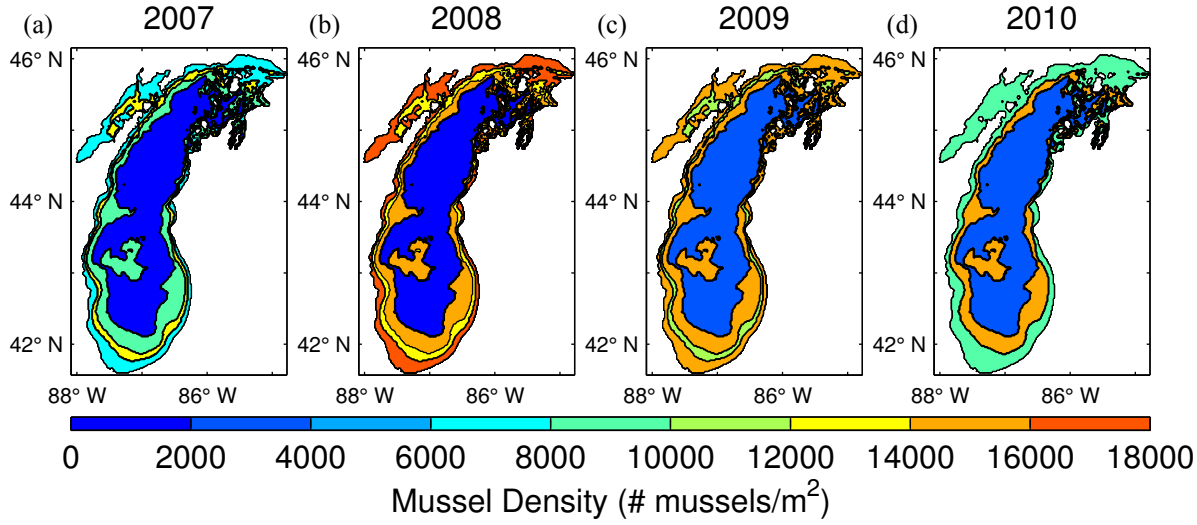
(a)
2007
(b)
2008
(c)
2009
(d)
2010
46° N
44° N
42° N
88° W
86° W
0
2000
4000
6000
8000
10000
12000
14000
16000
18000
Mussel Density (# mussels/m2)

Figure 4

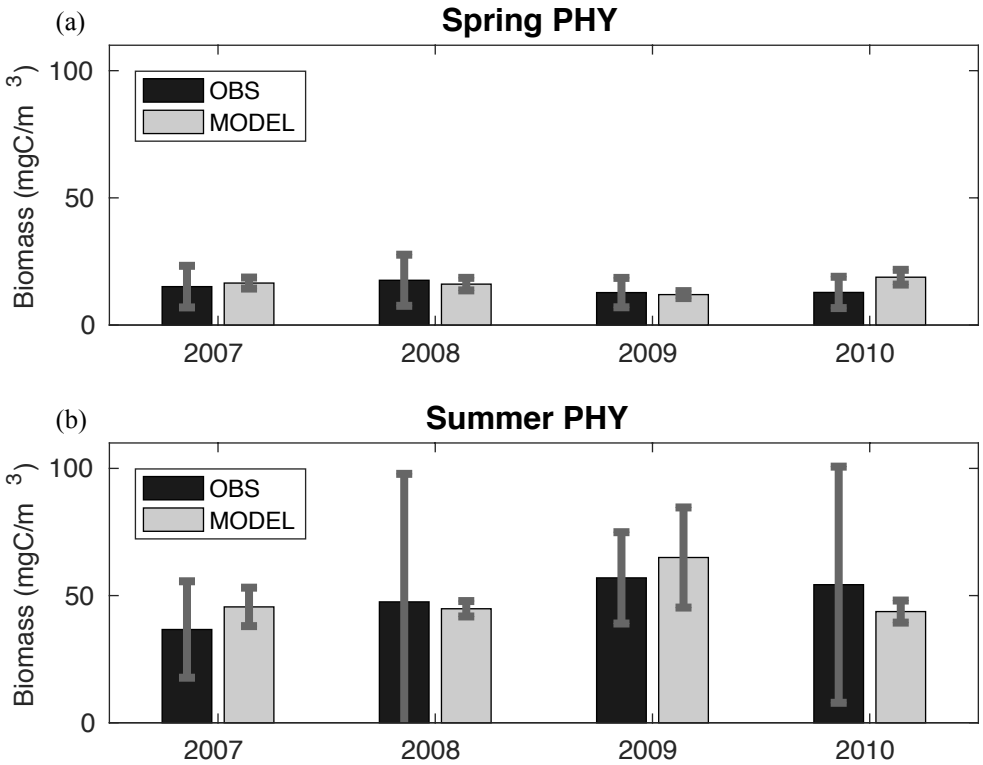
(a)
Spring PHY
Biomass (mgC/m 3)
100
50
0
OBS
MODEL
2007
2008
2009
2010
(b)
Summer PHY
Biomass (mgC/m 3)
100
50
0
OBS
MODEL
2007
2008
2009
2010

Figure 5

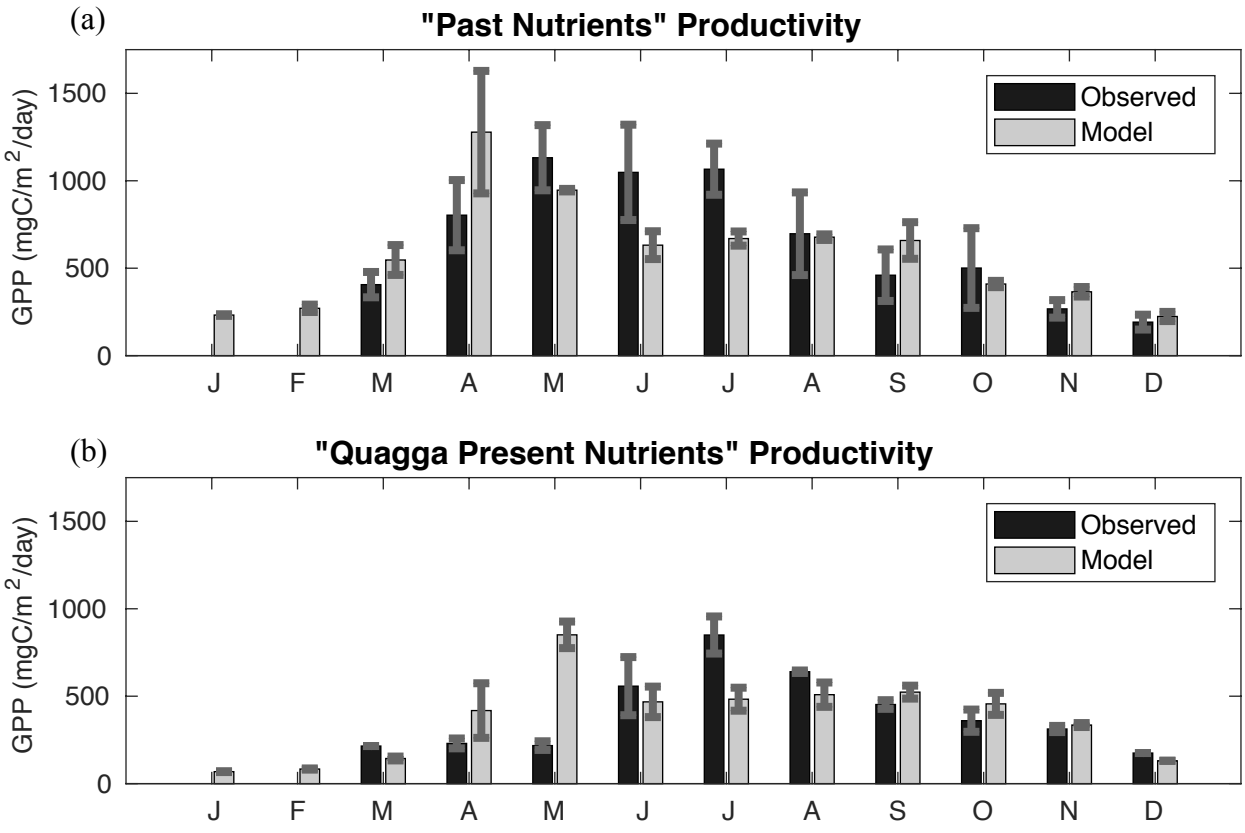
(a)
"Past Nutrients" Productivity
GPP (mgC/m 2/day)
1500
1000
500
0
Observed
Model
J F M A M J J A S O N D
(b)
"Quagga Present Nutrients" Productivity
GPP (mgC/m 2/day)
1500
1000
500
0
Observed
Model
J F M A M J J A S O N D

Figure 6

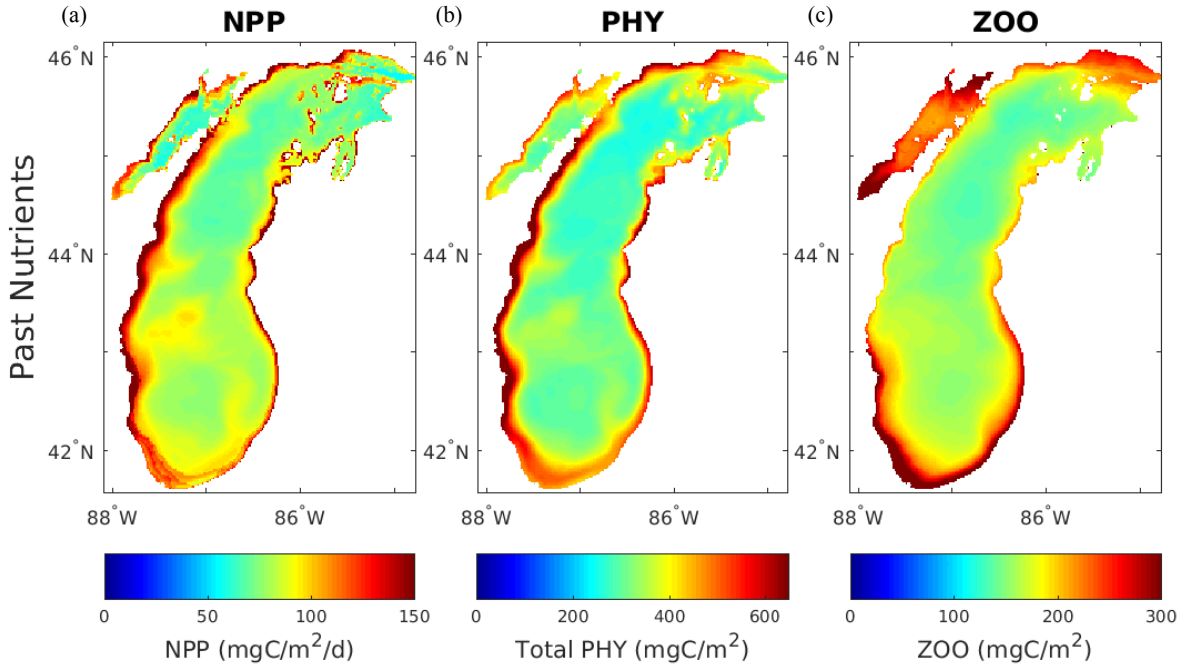
(a)
NPP
(b)
PHY
(c)
ZOO
Past Nutrients
46°N
44°N
42°N
88°W
86°W
0
50
100
150
NPP (mgC/m2/d)
0
200
400
600
Total PHY (mgC/m2)
0
100
200
300
ZOO (mgC/m2)

Figure 7

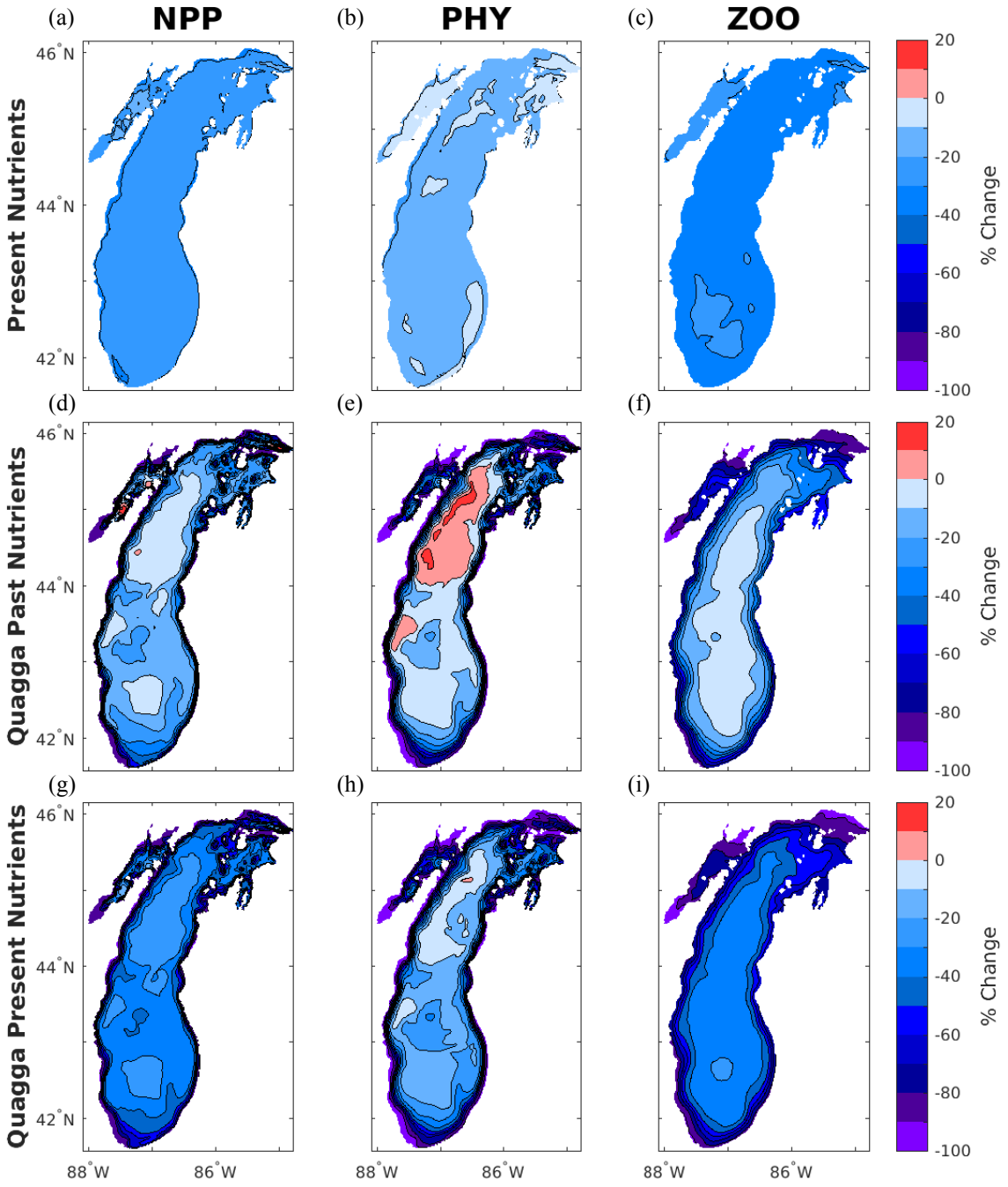
(a)
NPP
(b)
PHY
(c)
ZOO
Present Nutrients
(d)
(e)
(f)
Quagga Past Nutrients
(g)
(h)
(i)
Quagga Present Nutrients
46°N
44°N
42°N
88°W
86°W
20
0
-20
-40
-60
-80
-100
% Change

Figure 8

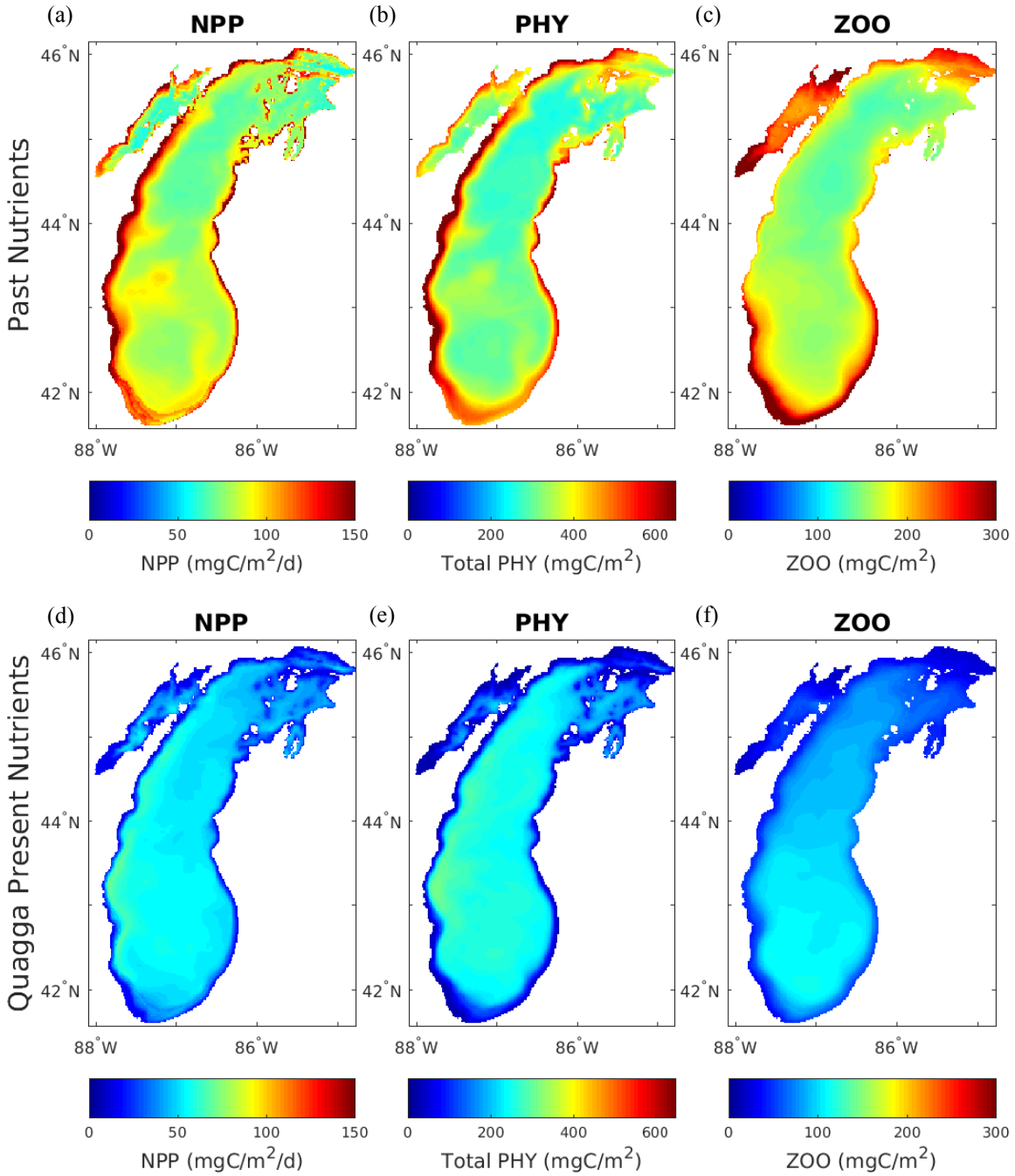
(a)
NPP
(b)
PHY
(c)
ZOO
Past Nutrients
46°N
44°N
42°N
88°W
86°W
0
50
100
150
NPP (mgC/m2/d)
0
200
400
600
Total PHY (mgC/m2)
0
100
200
300
ZOO (mgC/m2)
(d)
NPP
(e)
PHY
(f)
ZOO
Quagga Present Nutrients
46°N
44°N
42°N
88°W
86°W
0
50
100
150
NPP (mgC/m2/d)
0
200
400
600
Total PHY (mgC/m2)
0
100
200
300
ZOO (mgC/m2)

Figure 9

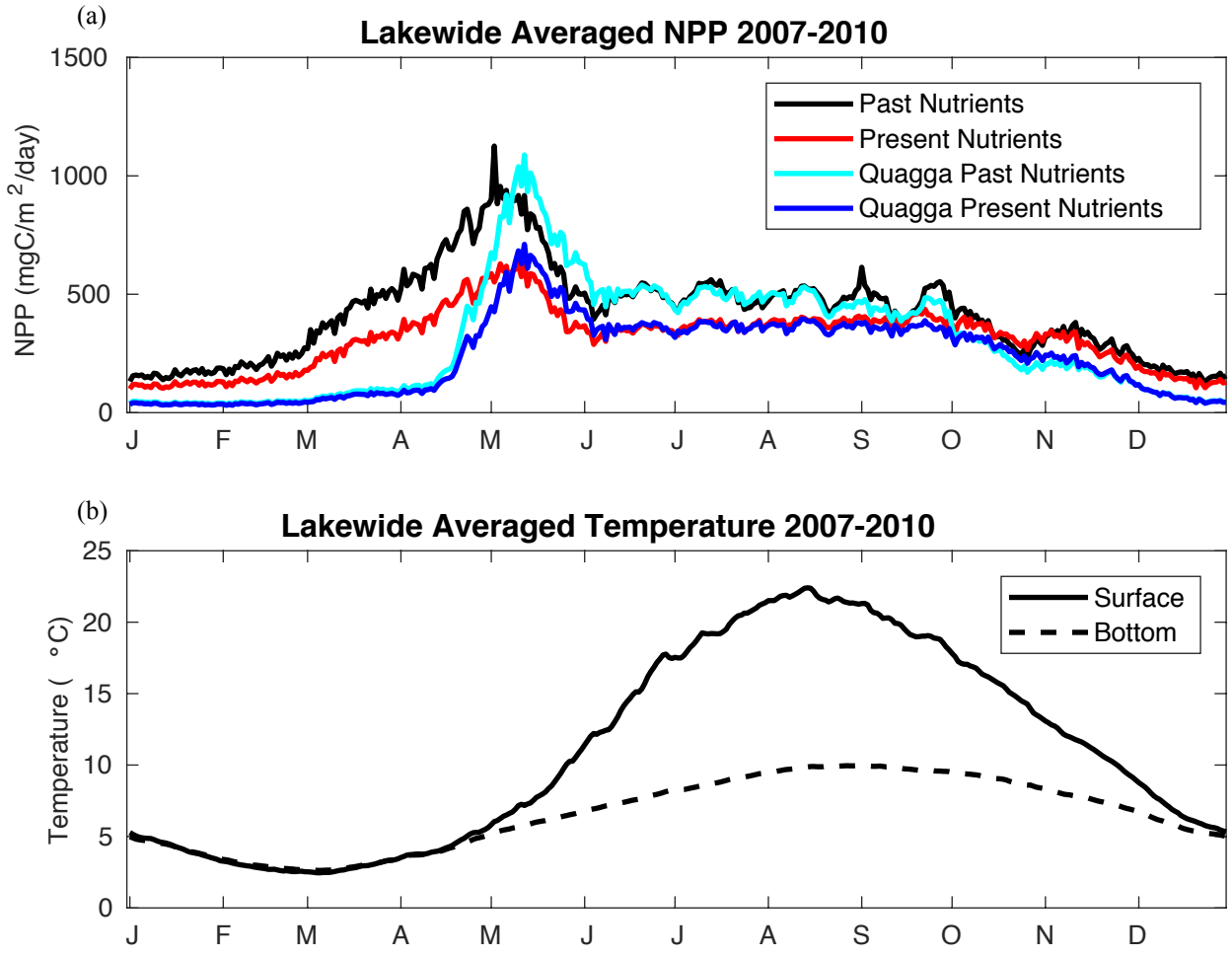
(a)
Lakewide Averaged NPP 2007-2010
NPP (mgC/m 2/day)
1500
1000
500
0
Past Nutrients
Present Nutrients
Quagga Past Nutrients
Quagga Present Nutrients
J F M A M J J A S O N D
(b)
Lakewide Averaged Temperature 2007-2010
Temperature (°C)
25
20
15
10
5
0
Surface
Bottom
J F M A M J J A S O N D

Figure 10

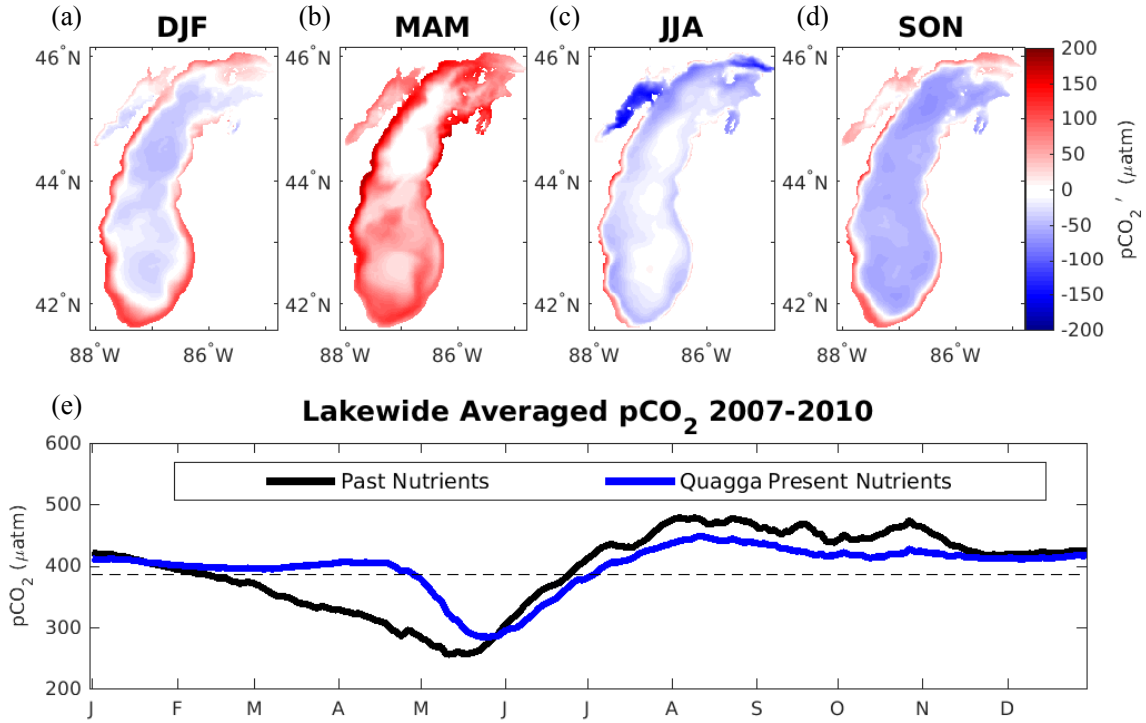
(a)
DJF
(b)
MAM
(c)
JJA
(d)
SON
46°N
44°N
42°N
88°W
86°W
200
150
100
50
0
-50
-100
-150
-200
pCO2′ (μatm)
(e)
Lakewide Averaged pCO2 2007-2010
Past Nutrients
Quagga Present Nutrients
pCO2 (μatm)
600
500
400
300
200
J
F
M
A
M
J
J
A
S
O
N
D

[Journal of Geophysical Research Biogeosciences]

Supporting Information for

[Modeled sensitivity of Lake Michigan productivity and zooplankton to changing nutrient concentrations and quagga mussels]

[Darren J. Pilcher [1,2], Galen A. McKinley [1,3,4], James Kralj [1,5], Harvey A. Bootsma [6], Euan D. Reavie [7]]

[[1] Department of Atmospheric and Oceanic Sciences, University of Wisconsin-Madison, Madison, WI, USA

[2] NOAA Pacific Marine Environmental Laboratory, Seattle, WA, United States

[3] Center for Climatic Research, University of Wisconsin-Madison, Madison, WI, USA

[4] Now at Columbia University / Lamont Doherty Earth Observatory, Palisades, NY 10964, USA.

[5] School of Marine and Environmental Affairs, University of Washington, Seattle, WA, USA

[6] School of Freshwater Sciences, University of Wisconsin-Milwaukee, Milwaukee, WI, USA

[7] Natural Resources Research Institute, University of Minnesota Duluth, Duluth, MN, USA]

Contents of this file

Introduction

The following supplementary information contains an expanded description of the model framework, including the implementation of quagga mussels and a discussion of the model sensitivity to the quagga mussel parameterization and C:P ratio. Also included are additional model validation figures and figures designed to complement the main text.

Text S1. *Additional Model Details*

MITgcm.Michigan is an eddy-resolving 3D model with approximate 2km horizontal resolution and 28 layers in the vertical. The model is forced by 3-hourly atmospheric downward shortwave and longwave radiation, 10m winds and air temperature, and specific humidity from the North American Regional Reanalysis Project (NARR) [*Mesinger et al.,* 2006]. Daily lake ice fraction is imposed from the U.S. National Ice Center [2010]. There is an established warm bias within the NARR forcing product that is greatest during colder years and also during spring stratification [*Bennington et al.,* 2010; *Pilcher et al.,* 2015]. The lake ice fraction can also generate a warm bias if the ice fraction is applied before the lake has cooled to 0°C, because this heat will be trapped over winter and released when the ice melts in early spring. Both of these factors contribute to a model warm bias that is greatest in the early spring, causing early thermal stratification.

Inorganic carbon is exchanged with the atmosphere based on the difference between the surface water partial pressure of CO_2 (pCO_2) of the lake and the atmosphere, with the carbon flux modified by the wind speed. Due to the short timeframe (2007-2010), atmospheric pCO_2 is kept at a constant value of 385 µatm. Lake pCO_2 is calculated from temperature, alkalinity, and dissolved inorganic carbon (DIC) following *Lewis and Wallace* [1998]. We use a quadratic relationship to parameterize the wind speed [*Wanninkhof* 1992]. Lake ice inhibits CO_2 exchange between the lake and atmosphere based on the percentage of the grid cell that is ice covered (i.e. a 40% coverage reduces the flux by 40%). Allochthonous inputs and burial of carbon are not included in the model implementation.

The model initial conditions are uniform in all three spatial dimensions, and are identical to the initial values in *Pilcher et al.,* [2015], with the exception of the initial phosphorus and

silicon concentrations, which are dependent on the model experiment. The model is spun-up with two consecutive years of 2007 forcing to achieve a repeating seasonal cycle in physical and biogeochemical fields, before running the full 2007-2010 timeframe.

Text S2. *Quagga Mussel Forcing*

Nalepa et al., [2010] report mean values from 40 stations located in the southern basin of Lake Michigan taken during the summer/fall from 1992-2008. *Nalepa et al.,* [2014] report mean values from up to 160 stations distributed lake-wide in 1994-95, 2000, 2005, and 2010. Because the two datasets contain different spatial and temporal resolutions, we combine them into a single product using the 2006-2008 data from *Nalepa et al.,* [2010] and the 2010 data from *Nalepa et al.,* [2014]. The resulting values are shown in Table S1. For consistency with the 2006-2008 values, we only utilize the same 40 stations from the 2010 dataset to generate the 2010 values shown in Table S1. The difference between using all stations and the 40 southern basin stations is negligible between two of the depth intervals, but yields 30% fewer mussels in the 31-50m range and 225% more mussels in the > 90m depth range. While the difference in the latter is substantial, we note that the reported uncertainty for that depth interval in 2010 is nearly 50% of the mean value. Furthermore, the difference between replicate samples in the raw data reported by *Nalepa et al.,* [2014] can be greater than an order of magnitude, illustrating the considerable uncertainty associated with sampling.

Quagga mussel filtration rates can vary between 0.25 – 9.6 L/mussel/day, due to mussel size, food source, species, and temperature [*Diggins* 2001; *Baldwin et al.,* 2002; *Vanderploeg et al.,* 2010]. We chose a fixed rate of 5.4 L/mussel/day because this rate falls near the middle of this range and is comparable to spring quagga filtration rates reported by *Diggins et al.* [2001].

Rowe et al., [2015a] in their model study use a fixed rate of 9.2 L/mussel/day for temperatures greater than 7°C, and a variable rate of ~ 2.1-9.2 L/mussel/day for temperatures between 1-7°C, based on a linear temperature dependence from *Vanderploeg et al.,* [2010]. Based on this temperature dependence, water temperatures near 4°C will yield a similar mussel filtration rate between our model and the model from *Rowe et al.,* [2015]. This is noteworthy considering that bottom water temperatures are often near 4°C in winter and early spring when the impact of quagga mussel grazing is greatest [*Fahnenstiel et al.,* 2010; *Rowe et al.,* 2015a; *Pilcher et al.,* 2015]. Overall, our filtration rates will be comparatively greater at colder water temperatures, but lesser at warmer water temperatures.

Text S3. *Model Sensitivity to Quagga Mussel Forcing*

Uncertainty in our mussel implementation is generated by (1) variance in mussel filtration rates, (2) variance in mussel size, and (3) spatial heterogeneity in mussel population density. However, quantifying these uncertainties requires either extensive observational data that is currently unavailable (e.g. spatial heterogeneity) or considerable computational costs associated with re-running multiple model simulations using different parameterizations (e.g. mussel rates and size vs. density). To get a first-order approximation of how this uncertainty impacts our results, we can compare productivity between model simulations with and without quagga mussels. We can further bin these results into the 4 depth intervals used to distribute mussel population density (Table S1), to determine the impact of varying mussel population numbers. Figure S1 shows the percent decrease in lakewide mean NPP due to the addition of quagga mussels, for each year and at each depth interval. There is a clear gradient of a greater decrease at shallow locations compared to deep locations, however this gradient does not

coincide with the gradient in mussel population densities. For example, the mussel population density from 2008-2010 is greater between 51-90m than between 31-50m, but this is not reflected in the total percent decrease in NPP (Figure S1). Furthermore, there are instances where mussel density increases but the impact to NPP decreases. At depths >90m, mussel density increases from 2009-2010, but the impact to NPP is reduced. This decrease in NPP is with respect to the same model year and atmospheric forcing, thus the only difference will be due to the mussels.

The purpose of Figure S1 is to illustrate that the variance in mussel population density tends to have a <10% impact on the total decrease in NPP. For example, a factor of 4 increase in mussel population at depths ≤ 30m between 2007-2008 generates a ~10% greater decrease in NPP. This factor of 4 difference is roughly half the variance in observed mussel filtration rates (0.25 – 9.6 L/mussel/day) and is greater than the 50-71% difference in respiration rates that results from assuming a uniform size (18 mm "large" mussels) vs. accounting for size frequency distribution [*Mosley and Bootsma* 2015]. Additionally, this factor of 4 difference roughly encompasses the variance between our constant filtration rate and the variable rate from *Rowe et al.,* [2015]. The model sensitivity to quagga forcing appears to be more of a function of lake depth than mussel population density. Sensitivity to lake depth is not surprising given that this will impact the duration of time that phytoplankton will spend in contact with the lake bottom and the volume of water for mussels to clear.

Text S4. *Model Sensitivity to the C:P Ratio*

The use of a constant molar C:P ratio is a common simplification in 3D modeling studies [*Bennington et al.,* 2012; *White and Matsumoto* 2012; *Pilcher et al.,* 2015] due to the uncertainty

and complexity associated with implementing a variable ratio. Observed variability in C:P ratios has been linked to a multitude of variables, including organism type, nutrient condition and light conditions, and lake size [*Hecky et al.,* 1993; *Elser et al.,* 2000; *Sterner et al.,* 2008; *Hessen et al.,* 2012]. We conducted 2 sensitivity tests using different C:P ratios to determine the quantitative impact on model results (Table S2; Figure S7). The first test used a lower C:P ratio of 150 for diatoms, but the same value of 200 for small phytoplankton. The second test used a C:P value of 150 for diatoms but a value of 300 for small phytoplankton. This second test was specifically designed to simulate the effect of higher C:P ratios under nutrient limited conditions, such as during periods when the lake is stratified and small phytoplankton are more prevalent.

Reducing the C:P ratio for diatoms by 25% (i.e. 200 to 150) produces a 15-20% decrease in modeled carbon-based productivity and phytoplankton carbon biomass (Table S2). The effect is relatively consistent between the Past Nutrients and Quagga Present Nutrients simulations, though slightly less sensitive with the latter. Additionally, increasing the C:P ratio for small phytoplankton by 50% (i.e. 200 to 300) offsets a substantial portion of the decrease produced via a lower C:P ratio for diatoms and produces a net increase in the Quagga Present Nutrients simulation. This result illustrates that the model is more sensitive to the C:P ratio for diatoms than small phytoplankton because a factor of 2 greater change in the C:P ratio for small phytoplankton was required to produce approximately the same magnitude of change as for diatoms.

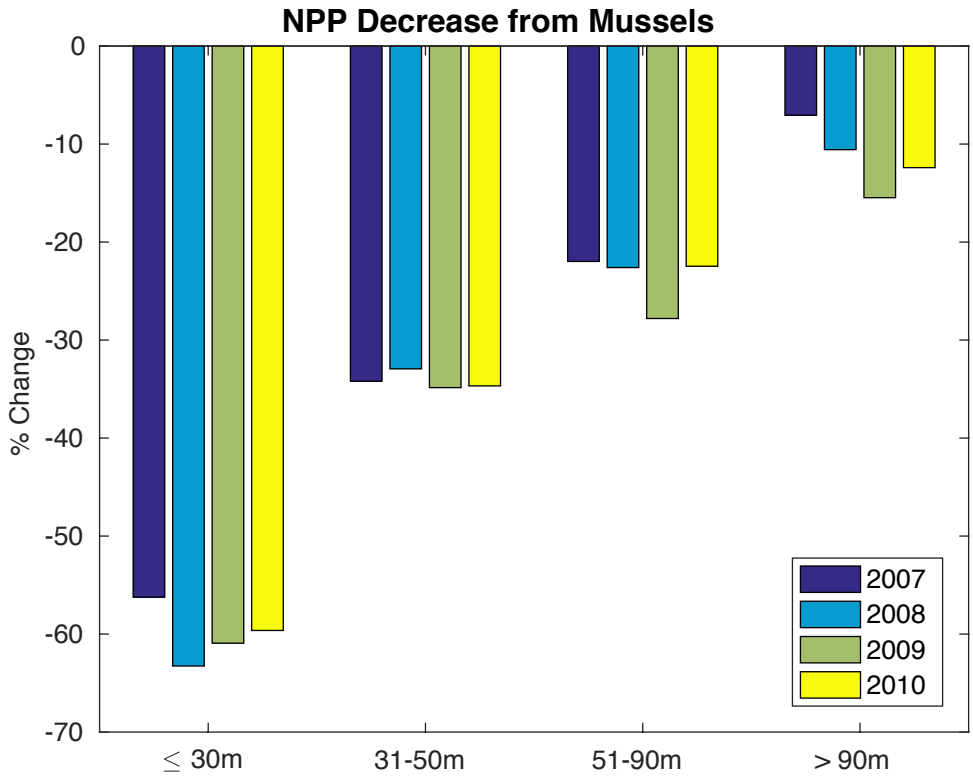

Figure S1. Bar plot showing the impact of quagga mussels on NPP for each simulation year and averaged over each depth interval used to map mussel population densities to lake depth. The magnitude of the bar is equal to the percent change in annual mean NPP between the Quagga Past Nutrients and Past Nutrients model simulations. Thus, a negative value indicates a decrease in NPP following the addition of quagga mussels.

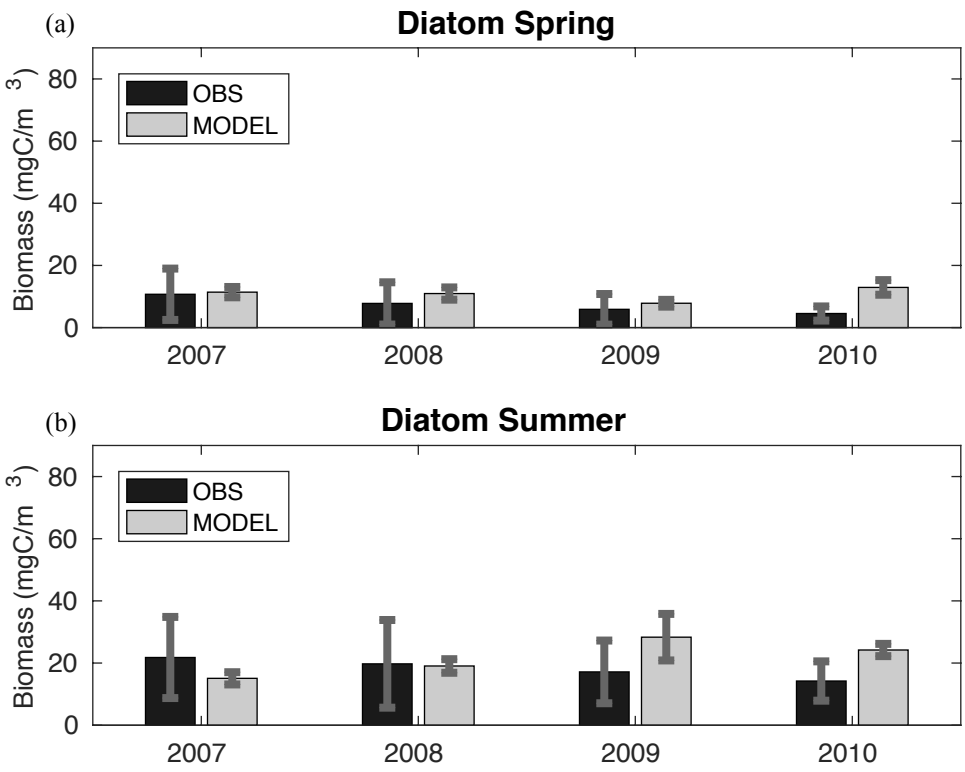

Figure S2. Spring (a) and summer (b) diatom biomass comparisons between the observations from the EPA Great Lakes Monitoring Program and the equivalent model locations. Shown is the average value across all 11 stations. The error bars signify the standard deviation across the stations. The observed diatoms include pennate and centric diatoms.

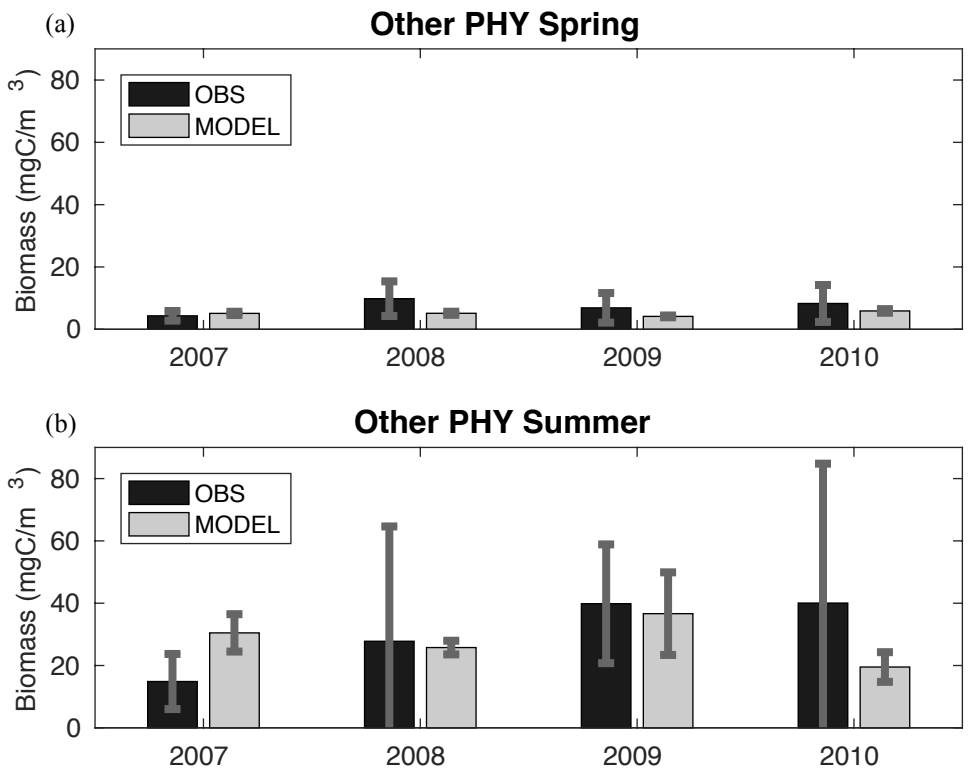

Figure S3. Spring (a) and summer (b) phytoplankton biomass comparisons between the observations from the EPA Great Lakes Monitoring Program and the equivalent model locations. Shown is the average value across all 11 stations. The error bars signify the standard deviation across the stations. Here, "other" phytoplankton consists of the non-diatom model phytoplankton group, and the combination of chlorophytes (green algae), chrysophytes, cryptophytes, cyanobacteria (blue-green algae), and pyrrophytes (dinoflagellates) for the observed phytoplankton.

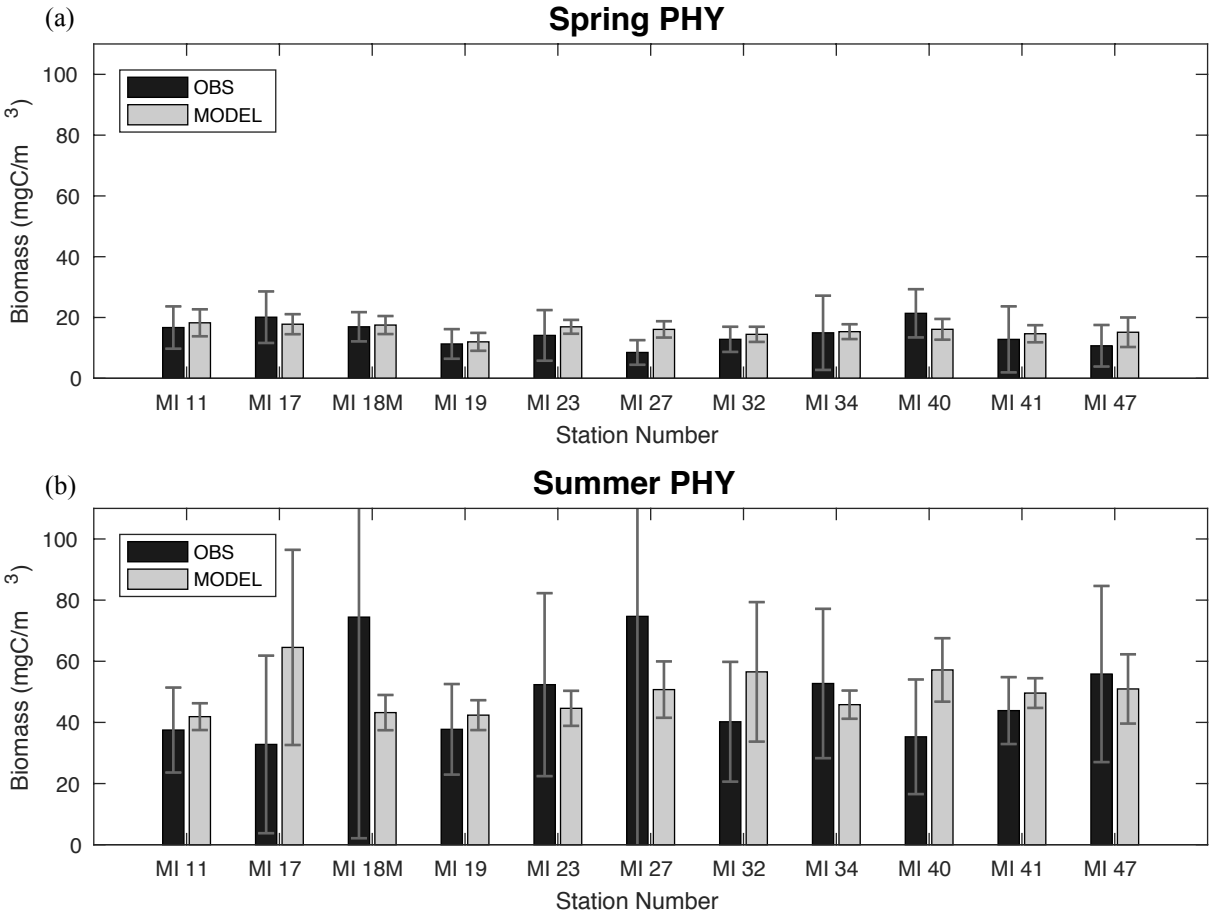

Figure S4. Spring (a) and summer (b) total phytoplankton biomass comparisons between the observations from the EPA Great Lakes Monitoring Program and the equivalent model locations. The error bars signify the standard deviation from 2007-2010.

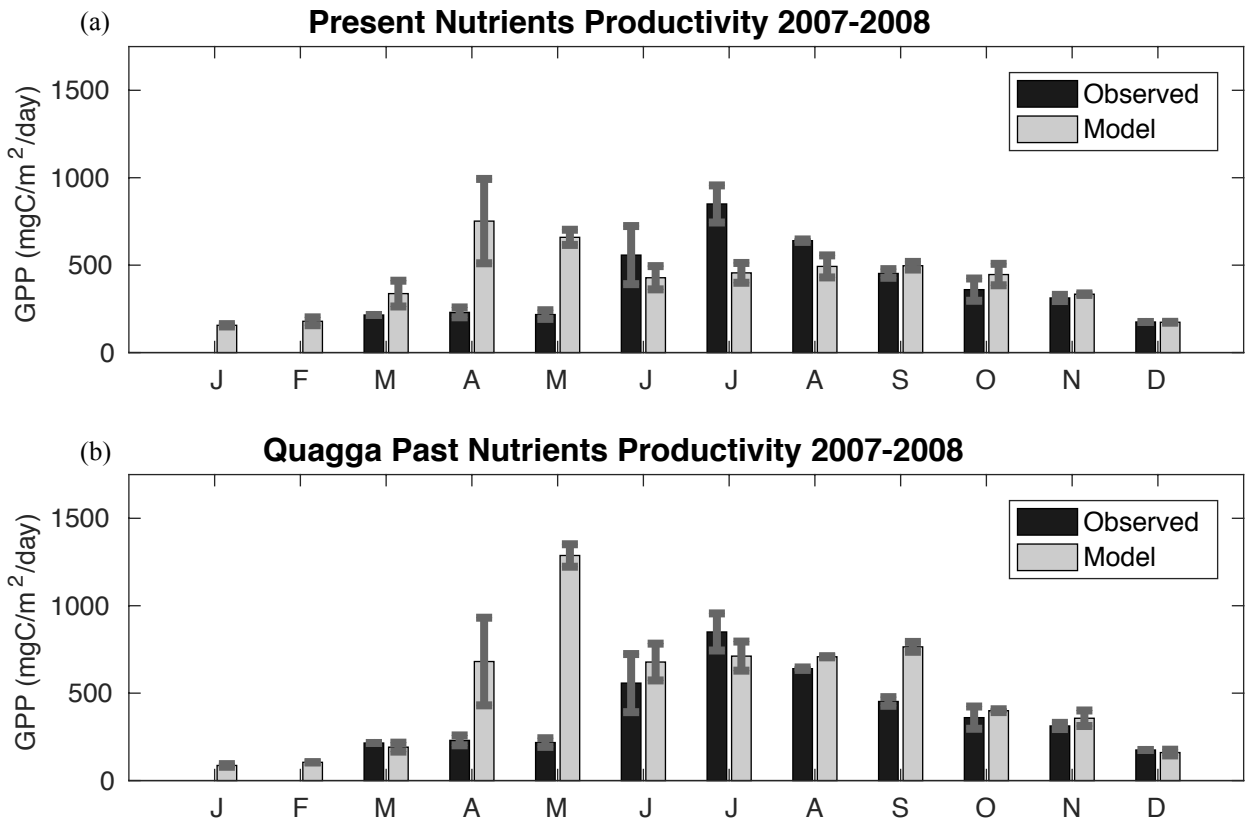

Figure S5. Comparison of model and observed GPP from *Fahnenstiel et al.,* [2010]. Model values come from the (a) Present Nutrients and (b) Quagga Past Nutrients simulations, and are averaged over the 2007-2008 forcing period. Error bars are the standard deviation over the timeframe. Note that there are no observed estimates for January and February.

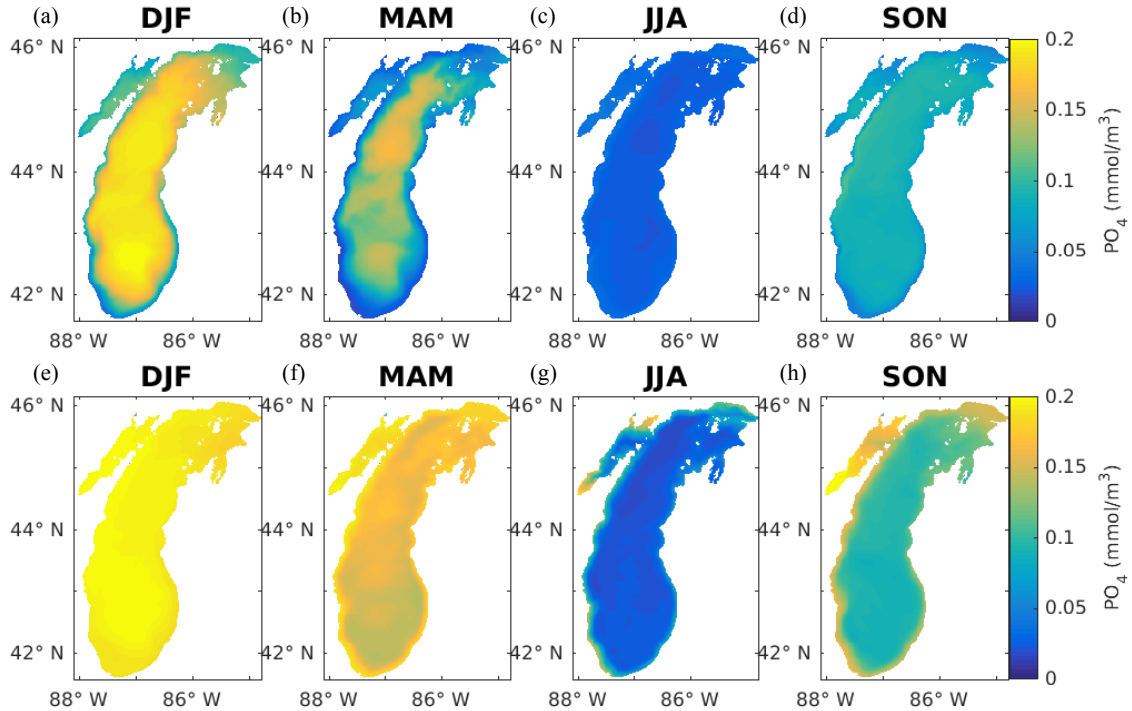

Figure S6. Seasonal spatial plots of 0-25m averaged phosphate concentrations in the (a-d) Present Nutrients and (e-h) Quagga Present Nutrients simulations. Shown is the 2007-2010 average.

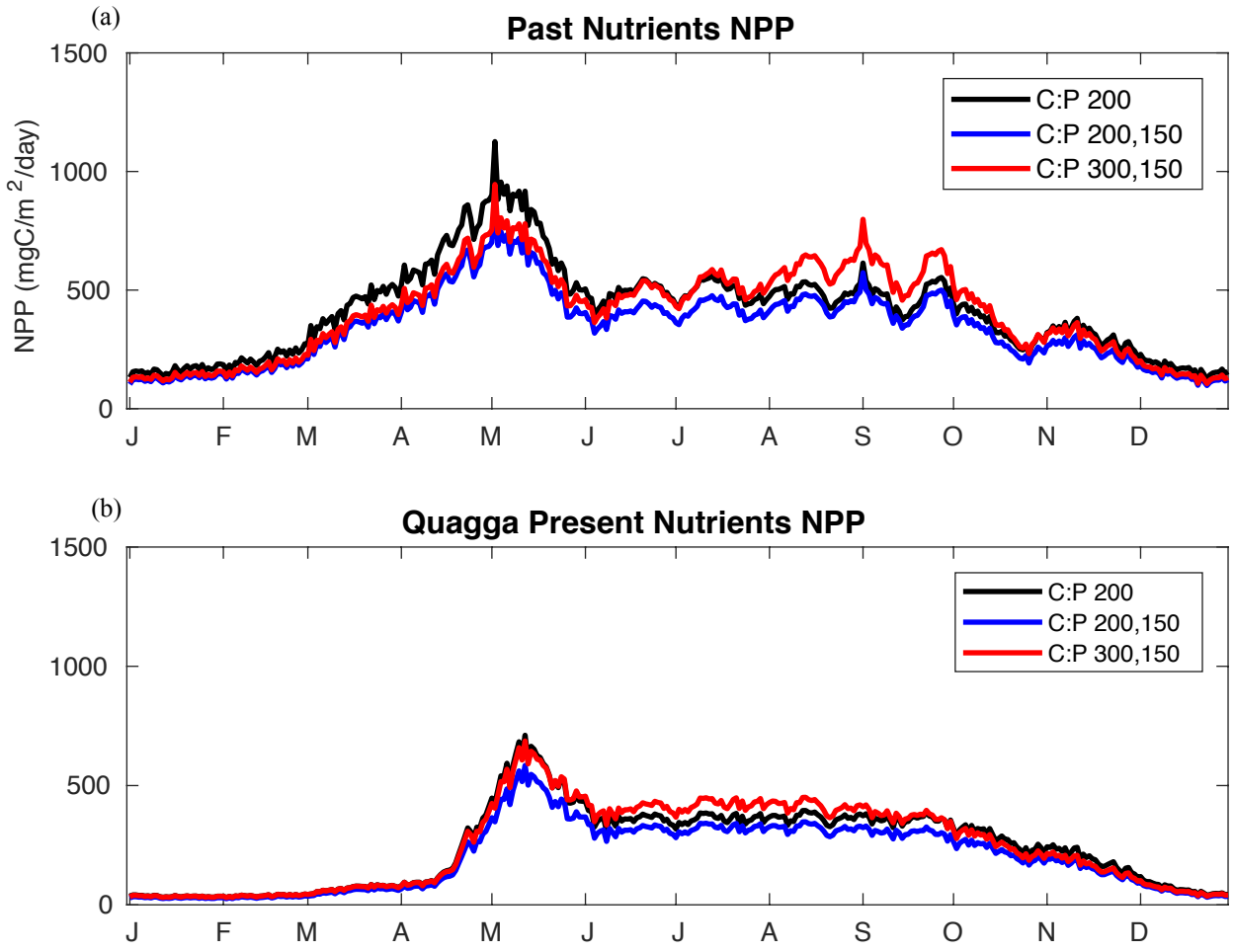

Figure S7. 4-year mean depth integrated NPP averaged over the entire lake for C:P sensitivity tests in the (a) Past Nutrients and (b) Quagga Present Nutrients simulations. The black line represents the constant C:P ratio used in the main analysis. The blue line represents the first sensitivity test using a C:P ratio of 200 for small phytoplankton but a C:P ratio of 150 for diatoms. The red line is the second sensitivity test using a C:P ratio of 300 for small phytoplankton and 150 for diatoms.

Depth Interval	**2006**[a]	**2007**[a]	**2008**[a]	**2010**[b]
≤ 30 m	12500	5000	20000	8679
31-50 m	13000	13000	12000	8867
51-90 m	4000	11000	15000	15122
> 90 m	400	800	2000	4223

Table S1. Quagga Mussel Densities

[a] Values estimated from Figure 2 of *Nalepa et al.,* [2010].

[b] Values calculated from *Nalepa et al.,* [2014].

PHY1 and PHY2 C:P Values	Past Nutrients NPP	Quagga Present Nutrients NPP	Past Nutrients PHY	Quagga Present Nutrients PHY
PHY1 C:P 200 PHY2 C:P 150	-15.1 (-17%)	-6.9 (-15.1%)	-70 (-19.2%)	-30.4 (-15.6%)
PHY1 C:P 300 PHY2 C:P 150	-0.8 (-1%)	2.2 (4.8%)	-27.8 (-7.6%)	6.0 (3.1%)

Table S2. Model sensitivity to C:P ratio. NPP is reported in units of $mgC/m^2/day$ and phytoplankton biomass is in units of mgC/m^2. The percent values represent the percent change compared to the respective model simulation using the constant C:P ratio of 200.